

Autonomous Two-Tier Cloud-Based Demand Side Management Approach with Microgrid

Mohammad Hossein Yaghmaee Moghaddam, *Senior Member, IEEE*,
 Morteza Moghaddassian, *Student Member, IEEE*, and Alberto Leon-Garcia, *Fellow Member, IEEE*

Abstract—Demand side management (DSM) is an important application of the future smart grid. DSM programs allow consumers to participate in the operation of the electric grid by reducing or shifting their electricity usage during peak periods. Therefore, in this paper, we propose a two-tier cloud-based DSM to control the residential load of customers equipped with local power generation and storage facilities as auxiliary sources of energy. We consider a power system consisting of multiple regions and equipped with a number of microgrids. In each region, an edge cloud is utilized to find the optimal power consumption schedule for customer appliances in that region. We propose a two-level optimization algorithm with a linear multilevel cost function. At the edge cloud, the power consumption level of local storage and the amount of power being demanded from both local storage facilities and power grid are scheduled by using a bi-level optimization approach. The core cloud then gathers information of the total demand from consumers in different Regions and finds the optimal power consumption schedule for each microgrid in the power system. Simulation results show that the proposed model reduces consumption cost for the customers and improves the power grid in terms of peak load and peak-to-average load ratio.

Index Terms—Cloud computing, demand side management (DSM), home energy management systems (HEMS), optimization, power consumption scheduling.

I. INTRODUCTION

THE smart grid (SG) uses two-way communications to gather the information from different parts of a power network. This information is used to monitor and control the generation, transmission, and distribution equipment. Information and communications technology (ICT) is the foundation of many applications in the SG. By utilizing ICT capabilities, the SG improves the efficiency, reliability, and sustainability of the power grid, and it delivers many benefits including efficient transmission of electricity, quick restoration of electricity

Manuscript received May 26, 2016; revised September 12, 2016; accepted October 9, 2016. Paper no. TII-16-0481. (Corresponding author: M. H. Y. Moghaddam.)

M. H. Y. Moghaddam is with the Department of Computer Engineering, Ferdowsi University of Mashhad, Mashhad 91779, Iran and also with the Department of Electrical and Computer Engineering, University of Toronto, Toronto M5S 3G4, ON, Canada (e-mail: hyaghmae@um.ac.ir).

M. Moghaddassian and A. Leon-Garcia are with the Department of Electrical and Computer Engineering, University of Toronto, Toronto M5S 3G4, ON, Canada (e-mail: m.moghaddassian@mail.utoronto.ca; alberto.leongarcia@utoronto.ca).

Color versions of one or more of the figures in this paper are available online at <http://ieeexplore.ieee.org>.

Digital Object Identifier 10.1109/TII.2016.2619070

after power disturbances, reduced operations and management costs for utilities, low power costs for consumers, reduced peak demand, increased integration of large-scale renewable energy systems, better integration of customer-owner power generation systems, and improved security.

Demand response (DR), which is one of most important applications of the SG, can be used in the future smart cities to inform consumers about their energy usage and costs. Smart consumers can make decisions autonomously about how and when to use electricity. By developing the Internet of Things (IoT) technology, it is possible to transfer customer's power consumption information to the cloud and develop a central demand side management (DSM) program to control and schedule the customer's appliances centrally. Without utilizing the SG applications, it is not possible to develop the smart cities. As described in [1], the IoT can be used to furnish intelligent management of energy distribution and consumption in heterogeneous circumstances. By leveraging the IoT-based appliances, the smart customers can send their optimal schedule to the utility companies. In the recent years, by the growth of IoT and digital technologies, smart cities have been becoming smarter than before.

In this paper, we propose a cloud-based DSM program that schedules the power consumption by customers in different regions and in microgrids so that both customer and utility company costs are optimized. There is a noticeable confluence between our proposed approach and the smart cities and IoTs, and that is the concept of service layer abstraction. More clearly, the proposed model can be implemented as an energy management component of the smart city that provides consumer electricity consumption management as a service. This concept defines many benefits including modularity in designing smart cities components and reducing the time and effort to extend the smart city services. Furthermore, it is designed to run on commodity hardware on a cloud computing platform, where the aggregation of hardware resources provides more power than any individual computing box. It can be considered as a data-driven model that can be further adjusted for any other utility management services. Cloud-based nature of the proposed model reduces the cost of computation that makes it easier for our future smart cities to deploy such services in future smart cities.

The cloud-based DSM utilizes the processing and storage resources of two-tier cloud computing consisting of the "Smart Edge" and the "Core cloud," to develop an optimal DSM. In our architecture, customers are classified into different regions. Each region is controlled by a "Smart Edge" cloud to provide cloud computing resources at the edge of the network precisely to meet low latency requirements as well as to

89 reduce the volume of traffic that needs to traverse the network
90 backbone. The core cloud performs a central optimization
91 at the multiregion level. At the customer side, consumption
92 information and local generation data are forwarded to an edge
93 cloud for the region. The edge cloud runs an optimization
94 process to find the optimal power consumption schedule for
95 both user appliances and local storage. After the edge cloud
96 obtains the optimal schedule for both appliances and local
97 storage devices, the total optimal load schedule of each region is
98 calculated and forwarded to the core cloud. The core cloud has
99 the load information for each region, and it also knows the
100 total stored energy in each microgrid. It can therefore perform
101 a centralized optimization to schedule the resource usage in the
102 microgrids so that the total multiregion cost is minimized. Our
103 main motivations for proposing a cloud-based DSM program are
104 as follows.

105 1) The single point of failure and the distributed denial-
106 of-service (DDoS) attacks from compromised nodes are
107 some significant concerns in the DR programs that are
108 based on master-slave architecture where the utility is
109 the master and customers are slaves. Although there are
110 solutions that are totally auto-reconfigurable and fault-
111 tolerant [2], but DDoS attack is still a big concern in
112 these approaches. By utilizing the cloud computing, the
113 proposed DSM model can decrease the negative effects
114 of DDoS attacks. The elastic nature of cloud comput-
115 ing allows it to provide the required communication and
116 computation resources, dynamically as needed especially
117 when a DOS attack happens. As the proposed DSM is
118 based on two-tier cloud computing, it can leverage the
119 existing defense method to prevent possible DDoS at-
120 tacks by rapidly provisioning resources when any attack
121 happens. The cloud-based DSM model can utilize some
122 popular methods against the DDoS attacks.

123 2) Current energy management systems that are used by
124 utilities to perform the DR programs suffer from lim-
125 ited memory and storage, especially, when the number
126 of customers is increased. By increasing the number of
127 customers in the system, to store the customer's data
128 and run the optimization process more computation and
129 storage resources are needed. In the cloud-based DSM
130 solution, as the optimization program is run at the cloud
131 server the memory and processing resources are always
132 available. When we need more resources (due to increase
133 in the number of customers or the size of optimization
134 problem), the cloud server can easily use some techniques
135 such as autoscaling to scale up the virtual machine and in-
136 crease its resources. Increasing the number of customers
137 in the optimization problem also increases the execution
138 time. So, we partition the problem into two parts edge
139 and core clouds which provides high scalability and fast
140 response time. Together these "edge clouds" and "core
141 clouds" create a multitier computing cloud. The motiva-
142 tions for these edge clouds certainly apply to SGs, and so
143 we explore the DSM in this multitier context. We utilize
144 the high processing and storage capabilities of multitier
145 cloud computing to run central optimization problems.

3) In the decentralized DSM, the optimization problem is
146 solved by the Energy Consumption Scheduler (ECS),
147 which is usually placed in the Home Energy Management
148 System (HEMS), or smart meter, which has limited com-
149 putational and capacity powers. In the distributed DSM
150 approaches, many iterations should be performed to find
151 the optimum solution. For example, for the distributed
152 DSM program given in [3] and for a power network with
153 100 users, when the channel bit error rate is 0.01 al-
154 most 10^6 update messages are exchanged to converge to
155 the optimal solution. In contrast, in the proposed cloud-
156 based DSM, all necessary calculations are performed at
157 the cloud servers provided by the utility companies. It
158 means that the users do not need to spend money to buy
159 sophisticated HEMS. They just need to participate in the
160 cloud-based energy efficient programs provided by the
161 utility companies or third party to optimize their energy
162 consumption.

163 4) In DSM programs based on the game theory (such as [3],
164 [4]), customers are classified in some clusters with dif-
165 ferent members. A local communications network needs
166 to be established between all customers. The assump-
167 tion that the customers have knowledge about their own
168 and the other customers' pay-offs is not practical. Fur-
169 thermore, techniques for solving games by using mixed
170 strategies, particularly for large pay-off matrix, are too
171 complicated. Unlike the decentralized DSM models, the
172 proposed work is based on the central optimization at the
173 cloud server. It means that the customers do not need to
174 communicate and cooperate together to find the optimal
175 solution. Entire operation is performed centrally at the
176 cloud server. We just need to collect the power consump-
177 tion information from all the customers and then run the
178 optimization problem. As the central server has a global
179 view of the power system, achieving an optimized solu-
180 tion is more feasible than the decentralized approaches
181 that are based on the local information.

182 5) When the power consumption scheduling is performed in
183 the distributed fashion, security is a big challenge. In the
184 distributed DSM, customers broadcast their local optimal
185 solutions. It has been proven that data broadcasting is not
186 secure. The hackers may access the ECS data, change
187 the users' consumption and scheduling information, and
188 broadcast fake data to other users in the same cluster.
189 Cloud computing offers a deployment architecture, with
190 the ability to address vulnerabilities recognized in the tra-
191 ditional information security. Cloud-based DSM can be
192 more secure than the decentralized DSM by using some
193 approaches such as multifactor authentication, security
194 patching, physical security, and security certifications.

195 6) Current grid technology suffers from peak loads that
196 arise from a drop in the supply or an increase in the
197 demand. It also limits the DR to static strategies, such
198 as time of use pricing and day-ahead notification based
199 on historical averages. In the proposed model, we
200 consider the photovoltaic (PV) based microgrid as an
201 auxiliary source of energy in our model and optimize it
202

so that the customer's cost could be minimized. Since microgrids are independent of the power grid, they can continue operating while the main grid is down. They can function as a grid resource for faster system response and recovery. Also, in the proposed model, the use of local sources of energy to serve local loads helps reduce energy losses in the transmission and distribution.

The rest of this paper is organized as follows. Section II, presents the literature review and background. In Section III, we explain the proposed model in detail. Section IV shows the simulation results that confirm the superior performance of the proposed model. Finally, Section IV concludes the paper.

II. LITERATURE REVIEW AND BACKGROUND

During past few years lot of research work has been devoted to DSM programs. There is now a rich literature on using optimization techniques and game theory to manage the demand at the customer side by minimizing the cost of power generation or maximizing the customers' utility [3]–[9]. Phase change materials (PCM) play a significant role in the future of buildings. PCM can be used for thermal energy storage system because simply it would be possible to include it into building components such as walls. In [10] by considering price-based and incentive-based DR programs, an optimized HEMS that employs the PCM for decreasing the residential demand and cost has been designed. As investigated in [10], when PCM is combined with the HEMS, the battery usage is reduced as compared to the case without PCM. In case of using PCM, most of the battery energy is utilized at the peak hour where the energy price is high. Dusparic *et al.* [11] define a decentralized DR approach that can be used to minimize the amount of residential power consumption, by maximizing the utilization of the generated power from wind energy resources. For a power system consisting of electric vehicles and wind renewable energy generators, the distributed W-Learning algorithm has been utilized. Each customer device is controlled by an intelligent agent that learns how to meet multiple goals and objectives. However, this approach suffers from some problems. First, distributed DR is based on the local objective function so finding the global solution especially when there are a lot of customers in the system is not possible. Second, cloud-based demand response (CDR) can utilize the autoscaling capabilities of cloud computing to adjust the necessary computation resources dynamically and provide more scalability and flexibility. The work in [12] for the customer homes with the time of use energy pricing, proposes two different DR and scheduling approaches including centralized and decentralized. In the decentralized mode, a microprocessor with a stand-alone algorithm is added to the smart plug (SP), to schedule the SPs optimally. However, adding microprocessor and related software to the SPs make them expensive for the customers. In the centralized approach, a central controller located at the HEMS, gathers the necessary information from the SPs to optimally schedule the SPs inside the home. However, this model does not consider the use of small power generation facilities and is not as broad as our model. Siano and Sarno [13] present a DR program considering the distribution locational

marginal price (D-LMP) energy market. It is supposed that customers can receive D-LMP price signal through the home gateway. The customers can join the real-time DR program by installing some specific equipment. The proposed optimization tries to maximize the benefit of the consumers and minimize the production cost of the producer. However, it just considers the fixed and shiftable loads and does not support the optimal scheduling of the local PV and microgrid in the model.

Recently, cloud computing has received attention for SG applications [14]–[16]. Most SG applications need reliable and efficient communications. This can be met by utilizing the cloud computing based on the software-defined infrastructure [17]. As investigated in [16] and [18], cloud computing brings some opportunities for SG applications. Flexible resources and services shared in the network, parallel processing, and omnipresent access are some features of cloud computing that are desirable for SG applications. Kim *et al.* [19] present the architecture of CDR which outperforms the previous work in terms of convergence speed while keeping the same messaging overhead.

III. PROPOSED MODEL

In this section, we present our proposed power system model and the cost function.

A. System Model

We assume that there are R different regions in the system. In each region r , there are m_r , $r \in \{1, \dots, R\}$ customers that are connected to the grid and consume energy. There are M distinct microgrids in the system. Each microgrid consists of distributed generation (DG) and distributed storage units. Without the loss of generality, we consider PV energy generation in each microgrid. We consider a two-tier cloud consisting of edge and core clouds. The edge cloud gathers the consumption (and also generation) information from all customers in each region and finds the optimal power consumption schedule for the customers so that the total energy consumption cost is minimized. Using existing data networks, the optimal consumption schedule is transferred to the HEMS. After all the edge clouds have calculated the optimal power consumption schedule of all customers in all regions, the total scheduled load information is transferred to the core cloud. The core cloud computes the total scheduled load gathered from the all edge clouds. Based on the total hourly load in the system, the core cloud schedules the optimal power consumption in each microgrid so that the peak-to-average ration (PAR) is decreased.

B. Power Consumers

We define three different types of power consumers.

- 1) *Type 0*: These are traditional power consumers. Type 0 consumers neither have local generation and storage nor the HEMS. It is not possible to schedule the power consumption for these consumers. These consumers do not require a data connection to the cloud. We consider these consumers as a variable hourly load in the power system that is not shiftable.

310 2) *Type 1*: These consumers have the HEMS, and two types
 311 of appliances, shiftable and nonshiftable. These con-
 312 sumers have a data connection to the cloud by using
 313 the HEMS. In order to minimize the power consumption
 314 cost and also reduce the PAR, the power consumption of
 315 shiftable appliances is scheduled.

316 3) *Type 2*: These are sophisticated consumers that are
 317 equipped with local generation and storage as well as the
 318 HEMS. When the main power grid is disconnected, which
 319 usually happens due to outages and the other source of
 320 blackout, the customers can use the local energy gen-
 321 eration and storage systems. These consumers generate
 322 part of their required energy by using PV systems. We
 323 assume that the generated power is stored in the local
 324 storage (battery) and is consumed by local appliances.

325 Let m_r^0 , m_r^1 , and m_r^2 denote the number of Type 0, Type 1, and
 326 Type 2 consumers, respectively, in region r , $r \in \{1, \dots, R\}$. As
 327 Type 0 consumers are not controllable, in the rest of this paper
 328 we consider just Type 1 and Type 2 consumers. For any cus-
 329 tomer n in region r , $n \in \{1, \dots, m_r\}$, $r \in \{1, \dots, R\}$, let $A_{r,n}$
 330 denote the set of appliances of this customer. We define $X_{r,n,a}$
 331 as the energy consumption scheduling vector, where $a \in A_{r,n}$
 332 denotes the appliance number and H is the scheduling horizon
 333 that indicates the number of hours ahead which are taken into
 334 account for decision making in energy consumption scheduling.
 335 We define $X_{r,n}$ vector as energy consumption scheduling vector
 336 for all appliances of customer n in region r . For Type 2 con-
 337 sumers, we define $P_{r,n} = \{p_{r,n}^1, p_{r,n}^2, \dots, p_{r,n}^h, \dots, p_{r,n}^H\}$, as
 338 the total power generation vector where $p_{r,n}^h$ denotes the amount
 339 of energy generated by the local PV system of customer n in
 340 region r at time h . In the next section, we will describe the
 341 proposed local generation model in detail.

342 The state of the charge (SOC) is one of the most important
 343 parameters for batteries that is defined as the ratio of its cur-
 344 rent capacity to the nominal capacity. The nominal capacity
 345 represents the maximum amount of charge that can be stored
 346 in the battery. The Coulomb counting method has been applied
 347 in order to estimate the SOC [20]. Suppose $\text{SOC}_{r,n}^h$ and $B_{r,n}^F$
 348 represent the SOC and the nominal battery capacity, respec-
 349 tively, of customer n in region r at time h . The current value of
 350 SOC ($\text{SOC}_{r,n}^h$) based on its previous value ($\text{SOC}_{r,n}^{h-1}$) and the
 351 charging/discharging current $I_b(t)$ is estimated as

$$\text{SOC}_{r,n}^h = \text{SOC}_{r,n}^{h-1} + \frac{I_b(t)}{B_{r,n}^F} \Delta t. \quad (1)$$

352 We define $B_{r,n} = \{b_{r,n}^1, b_{r,n}^2, \dots, b_{r,n}^h, \dots, b_{r,n}^H\}$, as the bat-
 353 tery state vector where $b_{r,n}^h$ denotes the amount of energy stored
 354 in the battery of customer n in region r at time h . Due to the lim-
 355 ited capacity of local storages, the following condition should
 356 be satisfied:

$$0 \leq b_{r,n}^h \leq B_{r,n}^F. \quad (2)$$

357 The value of $b_{r,n}^h$ is obtained by the following equation:

$$b_{r,n}^h = \text{SOC}_{r,n}^h \cdot B_{r,n}^F. \quad (3)$$

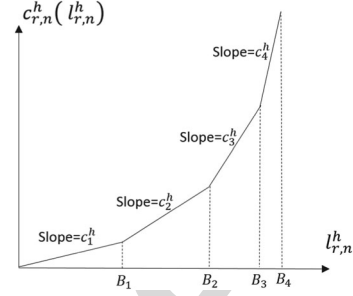


Fig. 1. Proposed N levels IBR pricing model.

358 Suppose $g_{r,n}^h$ and $y_{r,n}^h$ denote the amount of energy generation and consumption of Type 2 customer n in region r at time h . We assume that the customer consumes its available power in local storage first and then demands power from the power grid, if needed. We define $G_{r,n} = \{g_{r,n}^1, g_{r,n}^2, \dots, g_{r,n}^h, \dots, g_{r,n}^H\}$ and $Y_{r,n} = \{y_{r,n}^1, y_{r,n}^2, \dots, y_{r,n}^h, \dots, y_{r,n}^H\}$ as the power generation and consumption vector from the PV system, respectively. As the battery is charged by the solar energy ($g_{r,n}^h$) and is discharged by the local consumption ($y_{r,n}^h$), by combining (3) in (1) we have

$$b_{r,n}^h = b_{r,n}^{h-1} + g_{r,n}^h - y_{r,n}^h, \quad h = 2, \dots, H. \quad (4)$$

368 We define $l_{r,n}^h = X_{r,n}^h - y_{r,n}^h$ as the total hourly household energy consumption at each upcoming hour h . 369

C. Consumer Price Model 370

371 The proposed price model is designed by combining the real-time pricing (RTP) and inclining or increasing block rates (IBR) and considering N different blocks shown in Fig. 1. Our main objective of proposing this pricing model is to charge a higher rate per kilowatt-hour (kWh) at higher levels of energy usage and a lower rate at lower usage levels. The total cost of the customers who consume low energy (lower blocks) is less than those who consume more energy (higher blocks). The first block of B_1 kWh would cost c_1^h per kWh, the second block of B_2 kWh would cost c_2^h per kWh, and so on. Note that $c_i^h > c_{i-1}^h > 0$, $i \in \{2, \dots, N\}$, which means that the proposed pricing model charges a higher rate for each incremental block of consumption. To support the RTP, the price factors c_i^h are time dependent and may be changed hourly. For example suppose $N = 7$ and $B_i = i$ kWh. Based on the proposed pricing model the total power consumption cost for a customer with 6.5 kWh power consumption is computed as $(\sum_{i=1}^6 c_i^h + 0.5 c_7^h)$. Unlike the ToU and flat pricing, the introduction of IBR leads to energy savings. Another advantage of the proposed pricing is that it is straightforward and easy to understand by households. In the proposed pricing model, the cost of each block can be changed in real time. For each customer n in region r at time h , the power consumption cost $c_{r,n}^h (l_{r,n}^h)$ is calculated as follows (5) shown at the bottom of the next page. 399

396 It can be seen that the proposed cost function is increasing
397 and strictly convex. It means that

$$c_{r,n}^h(\hat{l}_{r,n}^h) < c_{r,n}^h(\tilde{l}_{r,n}^h), \quad \forall \hat{l}_{r,n}^h < \tilde{l}_{r,n}^h. \quad (6)$$

$$c_{r,n}^h(\varepsilon \hat{l}_{r,n}^h + (1 - \varepsilon) \tilde{l}_{r,n}^h) < \varepsilon c_{r,n}^h(\hat{l}_{r,n}^h) + (1 - \varepsilon) c_{r,n}^h(\tilde{l}_{r,n}^h). \quad (7)$$

398 As the proposed power system model is based on the hier-
399 archical model that consists of different regions, we can define
400 different price functions for different regions. This is because
401 each region is responsible for the power consumption optimiza-
402 tion of its customers. So, the proposed region-based optimiza-
403 tion allows us to take the geolocation of customers into account,
404 which helps us to prevent the possible congestion and peak
405 loading within particular regions. For instance, when a power
406 overload occurs at a particular region, the utilities may increase
407 the power price at that particular time at the specific region.
408 Thus, customers are encouraged to decrease their power con-
409 sumption or shift it to the nonpeak hours.

410 D. Distributed Power Generation Model

411 We suppose that PV systems are used for DG by Type 2
412 consumers and in microgrids. It has been proven that the total
413 energy generation by PV systems depends on parameters such
414 as temperature, total solar panel area, solar panel yield, and
415 performance of the installation including all losses (inverter
416 losses, temperature losses, dc and ac cables losses, shadings,
417 losses due to weak radiation, and losses due to dust and snow).

418 Previous studies [21]–[24] show that the power output of a
419 PV module depend linearly on the operating temperature. The
420 electrical performance is primarily influenced by the type of
421 PV used. A typical PV module converts 6–20% of the incident
422 solar radiation into electricity, depending upon the type of solar
423 cells and climatic conditions. The rest of the incident solar ra-
424 diation is converted into heat, which significantly increases the
425 temperature of the PV module and reduces the PV efficiency
426 of the module. To consider the effect of temperature in our PV
427 generation model, based on works given in [21] and [24], we
428 propose the following equation:

$$G_{pv} = A \cdot \mu \cdot \vartheta \cdot \tau_s \cdot (1 + \alpha (T_m - 25)) \quad (8)$$

429 where G_{pv} is the total annually energy generation (kWh), A
430 is the total solar panel area (m^2), μ is the solar panel yield
431 (default value %15), ϑ is the annual average irradiation on
432 tilted panels, which is changed regionally (between 500 and
433 2500 kWh/m².an), τ_s is the performance ratio and coefficient
434 for losses (default value %75), T_m is the temperature (in centi-
435 grade), and α is the temperature coefficient for power of the PV
436 module, which is $-0.20\%/^\circ\text{C}$.

437 Suppose $G_{h,d}^0$ represents the solar cell energy generation at
438 each hour h in day d when the sky is clear. When the sky is
439 cloudy, the energy generation is a portion of $G_{h,d}^0$ depending on
440 the cloud coverage. It is clear that the cloud coverage is related
441 to the time and the day of year. As it has been investigated
442 in [25], at each hour h in day d , the amount of solar energy
443 generation $G_{h,d}^F$ is calculated as follows:

$$G_{h,d}^F = K \cdot f(d) \cdot g(h) \cdot (1 - 0.75F_{h,d}^3) \quad (9)$$

444 where $F_{h,d}$ is the fraction of sky cloud cover on a scale from 0
445 (no clouds) to 1 (complete coverage) at time h of day d , K is a
446 normalization constant, and $f(d)$ and $g(h)$ are two functions
447 that indicate how much of the sun's power can be captured
448 in each hour for a particular day of the year. $f(d)$ is given as
449 follows [26]:

$$f(d) = \frac{\sin(90 - \varphi + \phi(d))}{\sin(90 - \varphi + \phi(d) + \theta)} \quad (10)$$

450 where φ and θ are latitude and the tilt angle of the module
451 measured from the horizontal, respectively. $\phi(d)$ is declination
452 angle calculated as [26]

$$\phi(d) = 23.45^\circ \cdot \sin\left(\frac{360}{365}(284 + d)\right). \quad (11)$$

453 The tilt angle has a major impact on the solar radiation in-
454 cident on a surface. For a fixed tilt angle, the maximum power
455 over the course of a year is obtained when the tilt angle is equal
456 to the latitude of the location ($\varphi = \theta$). We propose the flowing
457 Gaussian function for $g(h)$:

$$g(h) = e^{-\frac{(h-h_0)^2}{2\sigma^2}}, \quad h_0 = (t_{\text{sunset}} + t_{\text{sunrise}})/2 \quad (12)$$

458 where h_0 and σ^2 are the center and the variance of the Gaussian
459 function, respectively. t_{sunset} and t_{sunrise} are the sunset and
460 sunrise time, respectively. By substituting (10)–(12) into (9),
461 $G_{h,d}^F$ is obtained as follows:

$$G_{h,d}^F = K \frac{\sin(90 - \varphi + \phi(d))}{\sin(90 - \varphi + \phi(d) + \theta)} e^{-\frac{(h-h_0)^2}{2\sigma^2}} (1 - 0.75F_{h,d}^3). \quad (13)$$

462 As the total energy generation during all hours of all days in
463 a year should be equal to the annual energy generation, the
464 constant parameter K is obtained as follows:

$$K = \frac{G_{pv}}{\sum_{d=1}^{365} \sum_{h=1}^{24} \frac{\sin(90 - \varphi + \phi(d))}{\sin(90 - \varphi + \phi(d) + \theta)} e^{-\frac{(h-h_0)^2}{2\sigma^2}} (1 - 0.75F_{h,d}^3)}. \quad (14)$$

465 To investigate the accuracy of the PV generation model, we
466 compare the output of the PV generation model with that of the
467 3.15 kW PV system located in West Hobart, TAS, Australia [27],
468 and for date July 1, 2016. The real PV system generations were

$$c_{r,n}^h(l_{r,n}^h) = \begin{cases} c_1^h \cdot l_{r,n}^h & \text{if } B_0 = 0 \leq l_{r,n}^h \leq B_1 \\ \sum_{i=1}^{j-1} c_i^h \cdot (B_i - B_{i-1}) + c_j^h \cdot (l_{r,n}^h - B_{j-1}), j = 2, \dots, N-1 & \text{if } B_{j-1} < l_{r,n}^h \leq B_j \\ \sum_{i=1}^{N-1} c_i^h \cdot (B_i - B_{i-1}) + c_N^h \cdot (l_{r,n}^h - B_{N-1}) & \text{if } B_{N-1} < l_{r,n}^h \end{cases} \quad (5)$$

TABLE I
COMPARISON OF THE PV GENERATION MODEL WITH REAL DATA

Hour	8	9	10	11	12	13	14	15	16	17
Temperature	5.4	7.7	9.3	11.1	12	12.7	11.9	11.8	11.4	11.3
Real data	0.0	0.4	0.83	0.74	0.97	0.98	0.48	0.16	0.12	0.009
PV model	0.07	0.2	0.44	0.73	0.94	0.94	0.71	0.42	0.19	0.07

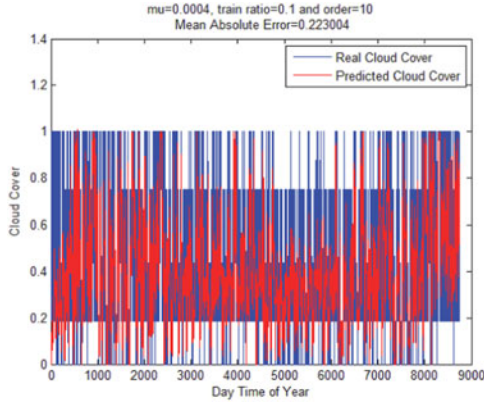


Fig. 2. Cloud coverage prediction efficiency (Toronto region, Jan. 1, 2015–Jan. 1, 2016).

469 measured and compared with the output of the proposed model.
470 The sunrise time, sunset time, and altitude of West Hobart, TAS,
471 were set to 8 A.M., 17 P.M., and 24 °S, respectively. The results
472 given in Table I, confirm that the proposed PV model has almost
473 0.13 mean absolute error.

474 E. Cloud Cover Prediction

475 Since the proposed model is based on a day-ahead optimization,
476 we have to know the amount of energy generation of the
477 Type 2 consumers and the microgrids in each hour of the next
478 day. For this purpose, we use (13), to evaluate the amount of
479 energy generation of PV systems for the next day. We also need
480 to estimate the cloud coverage $F_{h,d}$. The normalized least mean
481 square (NLMS) [28] predictor is the one providing the best
482 tradeoff between complexity, accuracy, and responsiveness. We
483 used the historical cloud coverage data given in [29] to tune the
484 filter parameters. The NLMS predictor needs the configuration
485 of two parameters: the order p and the step size μ . These param-
486 eters should be set correctly so that the best performance with
487 minimum error is obtained. In the case of the μ , it is relevant
488 to note that one of the main advantage of using NLMS is that
489 it is less sensitive to the step size with respect to other linear
490 predictor. In Fig. 2, at each hour of a day for the period of Jan. 1,
491 2015–Jan. 1, 2016 and for the Toronto city, the real cloud cover
492 and its prediction is plotted versus each hour of the day in the
493 year (totally $24 * 365 = 8760$ samples).

494 F. Edge Cloud Cost Optimization

495 As mentioned earlier, in each region there is an edge cloud
496 that gathers all the customers' consumption information to op-
497 timize the power consumption schedule. The optimal schedule
498 is obtained by the use of two-level optimization approach with
499 the predefined cost function as follows.

Level 1 optimization (for both Type 1 and Type 2 consumers):
In this stage the consumption pattern of all customer's shiftable
appliances in each region is scheduled by using the following
optimization problem:

$$\text{minimize } \sum_{h=1}^H c_{r,n}^h \left(\sum_{n=1}^{m_r} \sum_{a \in A_{r,n}} x_{r,n,a}^h \right)$$

Subject to

$$\alpha_a \leq x_{r,n,a}^h \leq \beta_a$$

$$\sum_{h=1}^H x_{r,n,a}^h = E_{r,n,a}$$

$$\gamma_{r,n}^{\min} \leq \sum_{a \in A_{r,n}} x_{r,n,a}^h \leq \gamma_{r,n}^{\max}$$

$$\text{Output : } x_{r,n,a}^* \quad (15)$$

where $E_{r,n,a}$ denotes the total energy needed for the operation
of appliance a of customer n in region r . α_a and β_a are the
beginning and end of a time interval, respectively, in which the
energy consumption for appliance a is valid, γ_a^{\min} and γ_a^{\max}
are the minimum and maximum power levels denoted of home
appliances. After optimization and thus rescheduling of shiftable
appliances, for each shiftable appliance a of customer n in
region r , the optimized energy consumption scheduling vector
 $X_{r,n,a}^*$ is obtained. By considering the nonshiftable and shiftable
appliances the optimal ECS vector $X_{r,n}^*$ for all appliances of
customer n in region r is obtained.

Level 2 optimization (only for Type 2 consumers): Type 2
consumers generate part of their energy consumption by using
the local generation such as the PV system. This energy is
stored in the batteries and consumed at the proper time. The
question is that to minimize the energy cost, what is the best
time for consuming this stored energy? To answer this question,
the following optimization problem is defined:

$$\text{minimize } \sum_{h=1}^H \sum_{n=1}^{m_r} c_{r,n}^h \left(x_{r,n}^{*h} - y_{r,n}^h \right).$$

Subject to:

$$\sum_{a \in A_{r,n}} x_{r,n,a}^{*h} \leq x_{r,n}^{*h},$$

$$\sum_{h=1}^H x_{r,n}^{*h} = \sum_{a \in A_{r,n}} E_{r,n,a}$$

$$0 \leq b_{r,n}^h \leq g_{r,n}^h$$

$$\sum_{h=1}^H g_{r,n}^h = \sum_{h=1}^H y_{r,n}^h$$

$$y_{r,n}^1 \leq b_{r,n}^1 \rightarrow b_{r,n}^1 = g_{r,n}^1$$

$$y_{r,n}^i \leq b_{r,n}^i \rightarrow b_{r,n}^i = b_{r,n}^{i-1} + g_{r,n}^i - y_{r,n}^{i-1}, i = 2, \dots, H$$

$$\text{Output : } y_{r,n}^* \quad (16)$$

Algorithm 1: Executed by each smart meter of Type 1 and Type 2 consumers.

- 1: **Randomly** initialize $x_{r,n,a}$ for Type 1 consumers and $G_{r,n}$, $B_{r,n}$ and $Y_{r,n}$ vectors for Type 2 consumers
 - 2: **Repeat**
 - 3: **At** random time instances **Do**
 - 4: **Send** vectors $x_{r,n,a}$ for Type 1 and Type 2 consumers and $G_{r,n}$, $B_{r,n}$ and $Y_{r,n}$ vectors for Type 2 consumers to the regional edge cloud server
 - 5: **if** changes happen to the vectors as a result of re/scheduling **Then**
 - 6: **Receive** optimized vectors $x_{r,n,a}^*$ for Type 1 and Type 2 consumers and $Y_{r,n}^*$ just for Type 2 consumers from the regional edge cloud server
 - 7: **Build** vector $X_{r,n}^*$ and **Update** the state of the consumer by building $l_{r,n}^*$ vector
 - 8: **End**
 - 9: **End**
 - 10: **Until** the meter is in service
-

522 where $x_{r,n}^{*h}$ is the optimal energy consumption obtained by the
 523 first optimization and is known. After the above-mentioned opti-
 524 mization problem is solved, the optimal power consumption
 525 vector $Y_{r,n}^*$ for local storages is obtained. The consumption load
 526 from the grid is obtained as $l_{r,n}^* = X_{r,n}^* - Y_{r,n}^*$. The optimiza-
 527 tion process in the edge cloud involves two important entities:
 528 smart meter and edge cloud server. The smart meter is involved
 529 for the purpose of power consumption information communi-
 530 cation while the edge cloud server is involved for running the
 531 optimization problem. The smart meter communication with the
 532 edge cloud server is explained in Algorithm 1. This algorithm
 533 is performed by smart meters for just smart consumers (Type 1
 534 and Type 2 consumers).

535 The algorithm for both level 1 and level 2 optimization in the
 536 edge cloud server is explained in detail in Algorithm 2. This
 537 algorithm is performed by each regional edge cloud for its own
 538 Type 1 and Type 2 consumers.

539 G. Core Cloud Cost Optimization

540 After optimization process is completed by each edge cloud,
 541 it sends its total hourly demand load vector to the core
 542 cloud. Each microgrid j , $j \in \{1, 2, \dots, M\}$ also sends vectors
 543 G_j , B_j , and Z_j to the core cloud, which represent the pre-
 544 diction of hourly power generation by microgrid, the remain-
 545 ing energy in the batteries, and the hourly power consumption
 546 level of each microgrid j , $j \in \{1, 2, \dots, M\}$, respectively. Let
 547 $L_h = (L^{th} - z^{th})$, denote the total hourly load in the power
 548 system where L^{th} is the total hourly demand load from all
 549 regions and z^{th} is the total hourly power consumption of all
 550 microgrids in the system are calculated as follows:

$$L^{th} = \sum_{r=1}^R \sum_{n=1}^{m_r} l_{r,n}^{*h} \quad (17)$$

$$z^{th} = \sum_{j=1}^M z_j^h. \quad (18)$$

Algorithm 2: Executed by each edge cloud.

- 1: **Repeat**
 - 2: **For** any Type 1 and Type 2 consumer in the region **Do**
 - 3: **Receive** vectors $x_{r,n,a}$ from any Type 1 and Type 2 consumers and $G_{r,n}$, $B_{r,n}$ and $Y_{r,n}$ vectors from any Type 2 consumers in the region
 - 4: **Solve** linear problem (15) using **IPM** (interior-point method)
 - 5: **if** changes happen to vector $x_{r,n,a}$ **Then**
 - 6: **Send** each vector $x_{r,n,a}^*$ to its corresponding consumers
 - 7: **End**
 - 8: **Solve** linear problem (16) using **IPM** (interior-point method)
 - 9: **if** changes happen to vector $Y_{r,n}$ **Then**
 - 10: **Send** each vector $Y_{r,n}^*$ to its corresponding consumers
 - 11: **End**
 - 12: **Build** $l_{r,n}^*$ vector and **Store** it in the local memory
 - 13: **End**
 - 14: **Build** the vector $l_r^{th} = \sum_{n=1}^{m_r} l_{r,n}^{*h}$ and **Send** it to the core cloud
 - 15: **Until** there is at least on consumer is in service
-

We consider the same linear multilevel cost function from (5) 552
 but with different cost coefficients. The following optimization 553
 problem is defined at the core cloud: 554

$$\text{minimize } \sum_{h=1}^H C_h(L_h) = \sum_{h=1}^H C_h(L^{th} - y^{th}). \quad (19)$$

Note that in the above optimization problem the value for 555
 L^{th} is fixed and is already calculated by edge clouds in the grid. 556
 Therefore, after running the optimization process at the core 557
 cloud, the optimized hourly consumption z^{t*h} from microgrid 558
 storages is obtained. The optimized total hourly load $L_h^* =$ 559
 $L^{th} - z^{t*h}$, which indicates the power consumption level from 560
 power grid, is obtained. The optimization algorithm is explained 561
 in detail in Algorithm 3. This algorithm is performed by the core 562
 cloud for all the entire grid after collecting the supporting data 563
 from all regional edge clouds and microgrids. 564

The operation of whole system is described by the flowchart 565
 given in Fig. 3. 566

567 IV. SIMULATION RESULTS

To compare the performance of the proposed model with that 568
 of the existing work, we consider a central version of work 569
 given in [3] without any Type 2 consumers and microgrids. We 570
 name it reference model. In the simulation model, we consider 571
 a power system that includes 5 regions with 2000 customers in 572
 each region. At each region, the percentage of Type 0, Type 1, 573
 and Type 2 consumers is 50, 30, and 20, respectively. For each 574
 customer we also consider 5–10 appliances with shiftable and 575
 nonshiftable operations. The initial parameters of all appliances 576
 are set by using data given in [30]. We also consider that each 577

Algorithm 3: Executed by the core cloud.

- 1: **Repeat**
- 2: **For** any microgrid $j \in M$ **Do**
- 3: **Receive** vectors G_j, B_j and Z_j
- 4: **End**
- 5: **Build** vector Z^t from the state vectors that have been sent by each microgrid
- 6: **Receive** vector $l_r^{t,h}$ from each edge cloud server
- 7: **Solve** linear problem (19) using IPM (interior-point method)
- 8: **If** changes happen to the optimization vectors in problem (19) **Then**
- 9: **Build** vectors Z^{t*} and L^* and **Update** the state of the grid
- 10: **End**
- 11: **Until** there is at least one edge cloud server or one microgrid in service

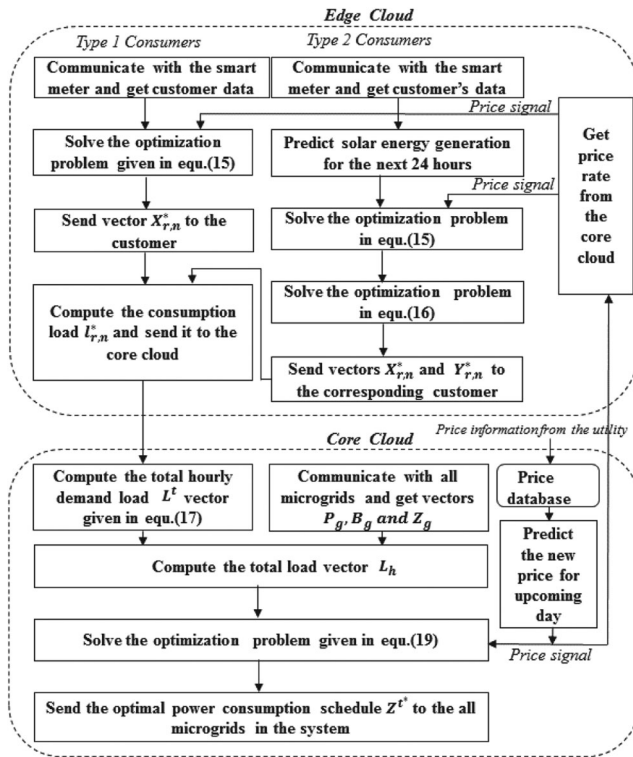


Fig. 3. Flowchart of whole process.

578 Type 2 customer is equipped with the average of 30 m² of
 579 photovoltaic cells. Similarly, we consider five microgrids with
 580 10 000 m² of solar cells for each. We suppose that the weather
 581 temperature for all solar cells is equal to 25 °C. We consider
 582 three different power usage intervals (12 A.M.–8 A.M., 8 A.M.–
 583 5 P.M., and 5 P.M.–12 A.M.) that correspond to off-peak, mid-
 584 peak, and high-peak hours of the day, respectively. The price of
 585 each kW power consumption at off-peak, mid-peak, and high-
 586 peak hours are supposed to be equal to 0.2, 0.3, and 0.5 cent,
 587 respectively. Then for each hour of the day we consider a seven-
 588 level pricing system that corresponds to the seven levels of load

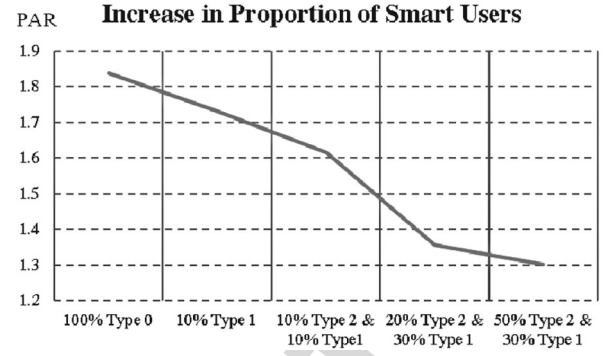


Fig. 4. Effects of the number of smart consumers on the PAR at different combinations of Type 0, Type 1, and Type 2.

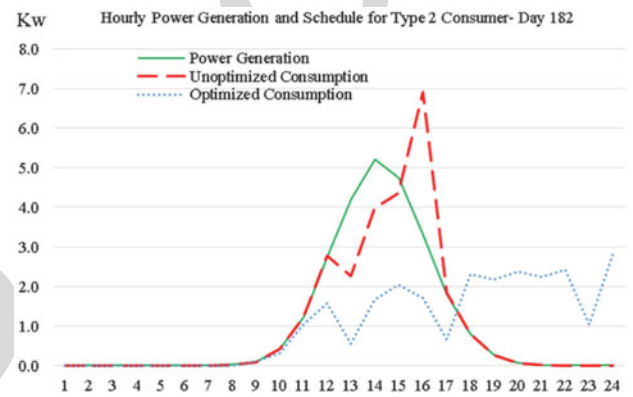


Fig. 5. Hourly power generation and consumption level from local storage facilities, a comparison between unoptimized and optimized approaches.

as defined before by the cost function. We consider the latitude of 589 Toronto, Canada, and set $\varphi = 43^\circ$ N. For the maximum energy 590 observation, we set the tilt angle of the module to the latitude as 591 $\theta = \varphi = 43^\circ$. We consider 31 days simulation interval between 592 Jul. 1 and Jul. 31, 2015 ($d \in [182, 212]$). The cloud coverage 593 data given in [29] are used for training the proposed predictor. 594 We also assume a daily time granularity ($H = 24$). This means 595 that the overall cloud solves the optimization problem for the 596 next 24 h. 597

In the first scenario, we investigate the effects of the number 598 of smart consumers (Types 1 and 2) on the performance of the 599 power system. The results given in Fig. 4 confirm that by 600 increasing the number of smart consumers, the PAR is decreased. 601 For example, when there are 50% Type 2 and 30% Type 1 602 consumers, we can achieve 0.52 decrease in PAR performance 603 comparing with the case that all consumers are Type 0. This 604 results from the higher number of sophisticated participants as 605 well as the higher number of DG resources available. 606

In Fig. 5, for a Type 2 customer and at day 182, the hourly local 607 power generation and usage from the battery (both unoptimized 608 and optimized scenarios) are depicted. It can be seen that almost 609 70% of the power consumption of the total generation of the 610 local PV system is shifted to the peak hours where the price of 611 the power is high. Therefore, the total cost and the amount of 612

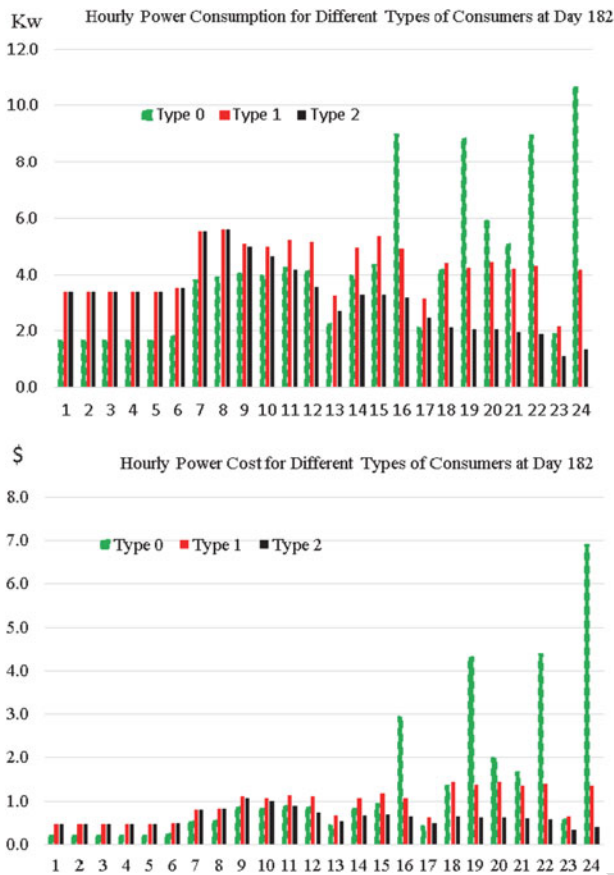


Fig. 6. Effects of smartness level on the hourly power consumption and cost.

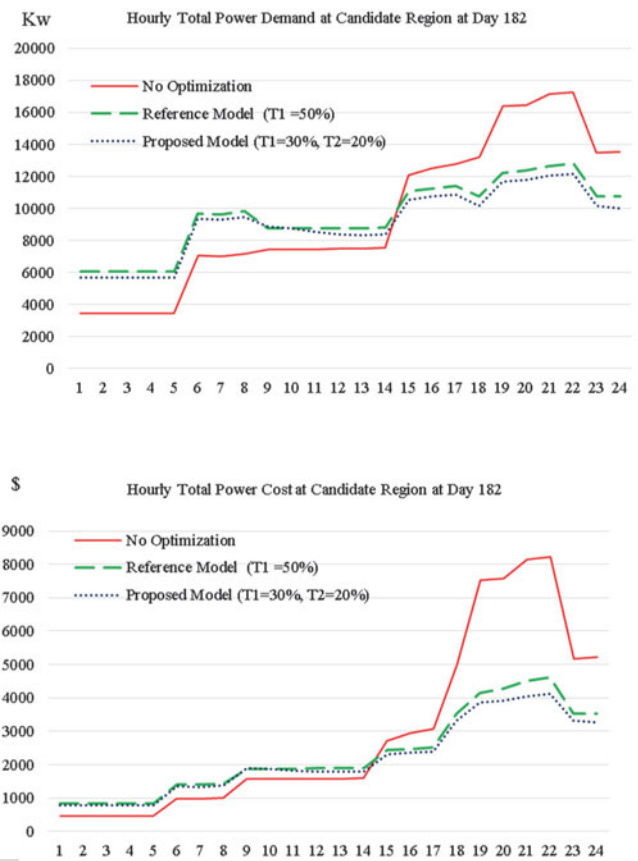


Fig. 7. Hourly power demand level and cost comparison for a candidate region.

power consumption from the power grid will be reduced and the grid will experience lower PAR.

In Fig. 6, for three candidates Type 0, Type 1, and Type 2 in a given region and at day 182, the hourly power consumption and the power cost are depicted. It can be seen that Type 2 consumers save 53.8% and 32.9% in power consumption cost in comparison to Type 0 and Type 1 consumers, respectively.

In Fig. 7, for a candidate region with 2000 customers, the hourly regional power demand level and costs are depicted. The figure illustrates a significant improvement from the no optimization case and the reference model [3]. It can be seen that in the case of both level 1 and level 2 optimizations (Proposed Model), the total daily cost can be reduced to 26.4% in comparison with the no-optimization case and 6.25% in comparison with the reference model [3], with regard to the percentage of Type 1 and Type 2 customers in the region.

In Fig. 8, for a power system with five microgrids, and for day 182, the amount of power generation in microgrids and power consumption schedule for the microgrid storage are depicted hourly. As the power usage from microgrids is stored in the battery and consumed at peak hours where the price is high, the results confirm that the optimized power consumption scheduling of the microgrid resources save almost \$1.04 per customer daily, in comparison with the unoptimized consumption. This helps to supply part of the customers' demands for electricity without

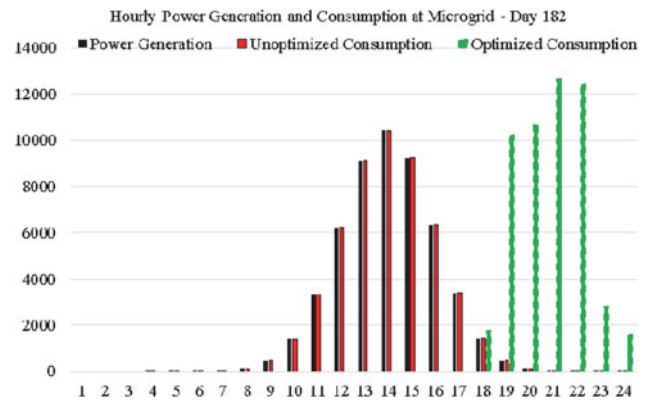


Fig. 8. Effects of the optimization on the hourly power consumption level in microgrids.

using grid resources at peak hours. Note that the black bar in Fig. 8 shows how much energy is generated by the microgrids at a particular day whereas the dash bar shows when and how much of this stored energy is consumed by the customers. This confirms that we store energy in the microgrid's battery during the daytime when the solar energy is high and then consume it at the peak hours when the demand and the energy prices both are high.

In Fig. 9, for two different cases of the proposed model (optimized and unoptimized), the performance of the total grid is evaluated. Optimized refers to the case that microgrid resources

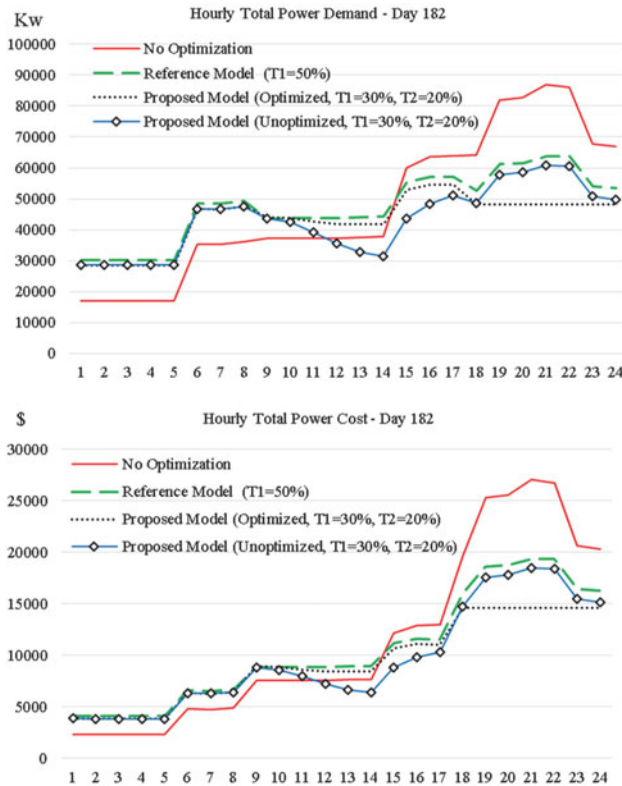


Fig. 9. Hourly grid demand level and costs comparison between no optimization, reference model [3], and the proposed model.

TABLE II
REGIONAL PAR COMPARISON, SHOWING THE IMPACTS OF ADDING MORE TYPE 2 CUSTOMERS

	All Type 0	Reference model [3] (50% Type 1)	Proposed model (30% Type 1, 20% Type2)	Proposed model (30% Type 1, 50% Type2)
Region number 1	1.82	1.35	1.34	1.2853
2	1.83	1.36	1.35	1.2860
3	1.86	1.36	1.35	1.2944
4	1.85	1.35	1.34	1.2880
5	1.83	1.33	1.32	1.2846

are used in the optimal way (after core cloud Algorithm 3 optimization) whereas unoptimized refers to using microgrid resources without any optimal scheduling. The results confirm that using microgrid with optimized scheduling (proposed model, optimized) can significantly improve the grid demand level and cost efficiency. For example, we can save 17.9% and 10.7% in total cost in comparison with no optimization and the reference model [3], respectively. We note that there are five microgrids in the whole grid that are assisted with 10 000 m² of photovoltaic cells, which are capable of generating almost 45 kW of electricity power during a day. By increasing the number of microgrids or the area microgrid solar cells, we can save more in cost and demand.

In Table II, we show that by adding more sophisticated customers (Type 2), the total regional PAR is decreased to a reason-

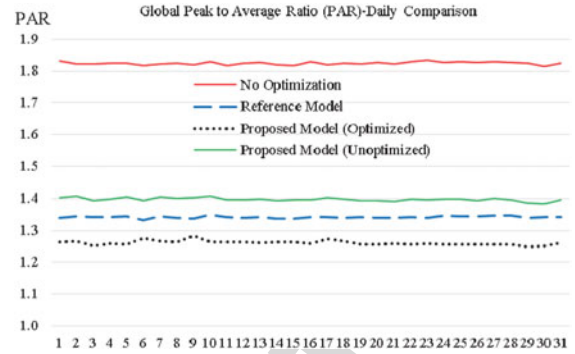


Fig. 10. Investigating the effects of using more sophisticated customers and using microgrids' power generation and storage facilities on the grid PAR.

able degree in comparison with the case of no smart customers (all Type 0). When the percentage of Type 2 consumers is low (20%), the difference between the proposed model and the reference model [3] is negligible. However, it can be seen that as Type 2 consumers place lesser demand on the overall grid, so by increasing the percentage of Type 2 consumers to 50%, the difference between the proposed model and the reference model [3] is increased slightly.

In Fig. 10, for four different approaches (no optimization, reference model [3], and optimized and unoptimized of the proposed model), the total PAR in the grid is plotted at different simulation days (from Jul. 1 to 31). As shown in Fig. 9, optimized refers to the case where microgrid resources are used in optimally (core cloud optimization), and unoptimized refers to use of microgrid resources without any optimal scheduling. It can be seen that using more sophisticated customers and microgrids with optimized power scheduling can significantly reduce the total PAR in the whole grid.

Finally, we investigate the scalability of the proposed model in terms of the convergence time of the optimization process time for different number of customers and regions. The execution time of the whole optimization process (including edge and core clouds) is measured. The proposed optimization is based on three different phases including collecting the information, running the optimization, and transferring the optimal schedule to the customers and microgrids. The optimization processing time directly depends on the performance of the cloud server and the number of customers and regions. When customers are spread in different regions, the required time for gathering information and running the optimization process decreases. By increasing the number of customers in the system, more computation and storage are needed to store the customer's data and run the optimization process. The simulation results show that increasing the number of customers in the optimization problem also increases the execution time. To avoid high execution time, we propose to partition the entire system into distinct regions and solve the optimization problem at each region, separately. Thus, high scalability and fast response time will be achieved. At the end of the optimization process, the optimal schedule is sent to the customers and microgrids. The results given in Table III confirm that 1) when the number of regions is fixed, by

TABLE III
PROCESSING TIME UNIT FOR RUNNING THE WHOLE OPTIMIZATION
PROCESS AT DIFFERENT COMBINATION OF CUSTOMERS AND REGIONS

		Number of regions			
		1	5	10	15
Number of customers in each region	500	NA	89.5062	90.7032	91.2865
	1000	NA	179.0042	179.6313	186.3749
	2000	NA	359.1821	360.4404	373.9718
	10 000	1764.2	NA	NA	NA
	20 000	3517.8148	NA	NA	NA

704 increasing the number of customers in each region the conver-
705 gence time is increased linearly and 2) when the total number
706 of customers in the whole power system is fixed, by increasing
707 the number of regions and spreading the customers in different
708 regions, the convergence time is decreased significantly.

709 V. CONCLUSION

710 The DSM needs reliable and efficient communications, which
711 can be met by utilizing the multitier cloud computing based on
712 the software-defined infrastructure. In this architecture, edge
713 cloud provides cloud computing resources at the edge of the
714 network. The benefit of such an architecture is that it can pro-
715 vide a high level of scalability and reliability. In this paper,
716 we proposed a two-tier cloud-based model for the autonomous
717 DSM in the future SG in which the customer's power consump-
718 tion and microgrid resources are scheduled by the use of the
719 regional edge and core clouds, respectively, to reduce the cost
720 and improve the power grid performance. It has been shown
721 that spreading the customers in different regions reduces the
722 convergence time and improves the scalability. As the proposed
723 approach is able to provide online access to all customer power
724 consumption information and microgrid resources, so it can en-
725 able the dynamic DR optimization of the power consumption
726 and energy cost of the customers. Simulation results confirmed
727 that the proposed model reduces the cost for the customers and
728 improves the power grid in terms of peak load and peak-to-
729 average load ratio.

730 REFERENCES

731 [1] H. Arasteh *et al.*, "IoT-based smart cities: A survey," in *Proc. 16th IEEE*
732 *Int. Conf. Environ. Electr. Eng.*, Florence Italy, 2016, pp. 1–6.
733 [2] A. M. Kosek, O. Gehrke and D. Kullmann, "Fault tolerant aggregation for
734 power system services," in *Proc 2013 IEEE Int. Workshop Intell. Energy*
735 *Syst.*, Vienna, 2013, pp. 107–112.
736 [3] A. H. Mohsenian-Rad, V. W. Wong, J. Jatskevich, R. Schober, and
737 A. Leon-Garcia, "Autonomous demand-side management based on game-
738 theoretic energy consumption scheduling for the future smart grid," *IEEE*
739 *Trans. Smart Grid*, vol. 1, no. 3, pp. 320–331, Dec. 2010.
740 [4] I. Atzeni, L.G. Ordóñez, and G. Scutari, "Demand-side management
741 via distributed energy generation and storage optimization," *IEEE Trans.*
742 *Smart Grid*, vol. 4, no. 2, pp. 866–876, Jun. 2013.
743 [5] S. Maharjan, Q. Zhu, Y. Zhang, S. Gjessing, and T. Basar, "Dependable
744 demand response management in the smart grid: A stackelberg game
745 approach," *IEEE Trans. Smart Grid*, vol. 4, no. 1, pp. 120–132, Mar.
746 2013.
747 [6] H. Chen, Y. Li, R. H. Y. Louie, and B. Vucetic, "Autonomous demand side
748 management based on energy consumption scheduling and instantaneous
749 load billing: An aggregative game approach," *IEEE Trans. Smart Grid*,
750 vol. 5, no. 4, pp. 1744–1754, Jul. 2014.

[7] R. Deng, Z. Yang, J. Chen, N. Rahbari-Asr, and M.Y. Chow, "Resi-
751 dential energy consumption scheduling: A coupled-constraint game ap-
752 proach," *IEEE Trans. Smart Grid*, vol. 5, no. 3, pp. 1340–1350, May
753 2014.
754 [8] D. Li and S. K. Jayaweera, "Distributed smart-home decision-making in
755 a hierarchical interactive smart grid architecture," *IEEE Trans. Parallel*
756 *Distrib. Syst.*, vol. 26, no. 1, pp. 75–84, Jan. 2015.
757 [9] D.S. Markovic, D. Zivkovic, I. Branovic, R. Popovic, and D. Cvetkovic,
758 "Smart power grid and cloud computing," *Renewable Sustain. Energy*
759 *Rev.*, vol. 24, pp. 566–577, 2013.
760 [10] M. Shafie-khah *et al.*, "Optimal behavior of responsive residential de-
761 mand considering hybrid phase change materials," *Appl. Energy*, vol. 163,
762 pp. 81–92, 2016.
763 [11] I. Dusparic, A. Taylor, A. Marinescu, V. Cahill and S. Clarke, "Maximizing
764 renewable energy use with decentralized residential demand response,"
765 in *Proc. 2015 IEEE First Int. Smart Cities Conf.*, Guadalajara, 2015,
766 pp. 1–6.
767 [12] L. C. Siebert *et al.*, "Centralized and decentralized approaches to demand
768 response using smart plugs," in *Proc. 2014 IEEE PES Transmiss. Distrib.*
769 *Conf. Expo.*, Chicago, IL, USA, 2014, pp. 1–5.
770 [13] P. Siano and D. Sarno, "Assessing the benefits of residential demand
771 response in a real time distribution energy market," *Appl. Energy*, vol.
772 161, pp. 533–551, 2016.
773 [14] A. Sheikhi, M. Rayati, S. Bahrami, A. M. Ranjbar, and S. Sattari,
774 "A cloud computing framework on demand side management game in
775 smart energy hubs," *Electr. Power Energy Syst.*, vol. 64, pp. 1007–1016,
776 2015.
777 [15] M. Yigit, V. C. Gungor, and S. Baktir, "Cloud computing for smart grid
778 applications," *Comput. Netw.*, vol. 70, pp. 312–329, 2014.
779 [16] J.-M. Kang, T. Lin, H. Bannazadeh, and A. Leon-Garcia, "Software-
780 defined infrastructure and the SAVI testbed," in *Testbeds and Research*
781 *Infrastructure: Development of Networks and Communities*. New York,
782 NY, USA: Springer, 2014, pp. 3–13.
783 [17] R. Deng, Z. Yang, M. Chow, and J. Chen, "A survey on demand response
784 in smart grids: Mathematical models and approaches," *IEEE Trans. Ind.*
785 *Inform.*, vol. 11, no. 3, pp. 570–582, Jun. 2015.
786 [18] S. Bera, S. Misra, and J. J. P. C. Rodrigues, "Cloud computing applications
787 for smart grid: A survey," *IEEE Trans. Parallel Distrib. Syst.*, vol. 26, no. 5,
788 pp. 1477–1494, May 2015.
789 [19] H. Kim, Y. J. Kim, K. Yang and M. Thottan, "Cloud-based demand
790 response for smart grid: Architecture and distributed algorithms," in
791 *Proc. 2011 IEEE Int. Conf. Smart Grid Commun.*, Brussels, 2011,
792 pp. 398–403.
793 [20] K. S. Ng, C. S. Moo, Y. P. Chen, and Y. C. Hsieh, "Enhanced coulomb
794 counting method for estimating state-of-charge and state-of-health of
795 lithium-ion batteries," *Appl. Energy*, vol. 86, no. 9, pp. 1506–1511,
796 2009.
797 [21] J. Hofierka and J. Kaňuk, "Assessment of photovoltaic potential in urban
798 areas using open-source solar radiation tools," *Renew. Energy* vol. 34,
799 no. 10, pp. 2206–2214, Oct. 2009.
800 [22] C. Koch-Ciobotaru, L. Mihet-Popa, F. Isleifsson and H. Bindner, "Simu-
801 lation model developed for a small-scale PV system in distribution net-
802 works," in *Proc. 2012 7th IEEE Int. Symp. Appl. Comput. Intell. Inform.*,
803 Timisoara, 2012, pp. 341–346.
804 [23] R. G. Ross, "Flat-plate photovoltaic array design optimization," in *Proc.*
805 *14th IEEE Photovolt. Spec. Conf.*, 1980, pp. 1126–1132.
806 [24] K. Nishioka, T. Hatayama, Y. Uraoka, T. Fuyuki, R. Hagihara, and
807 M. Watanabe, "Field-test analysis of PV system output characteristics
808 focusing on module temperature," *Solar Energy Mater. Solar Cell*, vol.
809 75, no. 3–4, pp. 665–671, 2003.
810 [25] F. Kasten and G. Czeplak, "Solar and terrestrial radiation dependent on
811 the amount and type of cloud," *Solar Energy*, vol. 24, no. 2, pp. 177–189,
812 1980.
813 [26] J. A. Duffie and W. A. Beckman, "*Solar Engineering of Thermal Pro-*
814 *cesses*," 4th ed. Hoboken, NJ, USA: Wiley, 2013.
815 [27] "Solar PV maps and tools," 2016. [Online]. Available: [http://pv-](http://pv-map.apvi.org.au/)
816 [map.apvi.org.au/](http://pv-map.apvi.org.au/)
817 [28] R. G. Garroppo, S. Giordano, M. Pagano, and G. Procissi, "On traffic
818 prediction for resource allocation: a Chebyshev bound based allocation
819 scheme," *Comput. Commun.*, vol. 31, no. 16, pp. 3741–3751, 2008.
820 [29] IEM, "Iowa Environmental Mesonet (IEM)," 2016. [Online]. Available:
821 <https://mesonet.agron.iastate.edu>
822 [30] Office of Energy Efficiency, Natural Resources Canada, Energy Con-
823 sumption of Household Appliances Shipped in Canada Trends for
824 1990–2010, 2016. [Online]. Available: [http://www.nrcan.gc.ca/sites/](http://www.nrcan.gc.ca/sites/oee.nrcan.gc.ca/files/pdf/publications/statistics/cama12/cama12.pdf)
825 [oee.nrcan.gc.ca/files/pdf/publications/statistics/cama12/cama12.pdf](http://www.nrcan.gc.ca/sites/oee.nrcan.gc.ca/files/pdf/publications/statistics/cama12/cama12.pdf)
826

827
828
829
830
831
832
833
834
835
836
837
838
839
840
841
842
843
844
845
846
847
848
849
850
851
852
853
854
855
856
857
858
859
860
861
862
863
864
865
866



Mohammad Hossein Yaghmaee Moghaddam (SM'12) received the B.S. degree from Sharif University of Technology, Tehran, Iran, in 1993, and the M.S. and Ph.D. degrees in communication engineering from Tehran Polytechnic (Amirkabir) University of Technology, Tehran, Iran, in 1995 and 2000, respectively.

From November 1998 to July 1999, he was with the Network Technology Group, C&C Media Research Labs., NEC corporation, Tokyo, Japan, as a Visiting Research Scholar. From

September 2007 to August 2008, he was with the Lane Department of Computer Science and Electrical Engineering, West Virginia University, Morgantown, WV, USA, as a Visiting Associate Professor. From July 2015 to September 2016, he was with the Electrical and Computer Engineering Department, University of Toronto, Toronto, Canada, as a Visiting Professor. Currently, he is a Full Professor at the Computer Engineering Department, Ferdowsi University of Mashhad, Mashhad, Iran. His research interests include SG communication, software defined networking, and network function virtualization.



Morteza Moghaddassian (S'15) received the M.S. degree in computer engineering from Ferdowsi University of Mashhad, Mashhad, Iran, in 2015. Since 2016, he is working toward the Ph.D. degree in electrical and computer engineering at the University of Toronto, ON, Canada.

He received the Edward S. Rogers Sr. departmental graduate fellowship. Prior to this, he was a Research Assistant at the Center of Excellence on Soft Computing & Intelligent Informa-

tion Processing, Ferdowsi University of Mashhad, Mashhad, Iran, where he successfully managed a research team to develop a social energy network application for the purpose of metering with built-in demand-response management modules, called "SocioGrid." His research interests include cloud computing, edge computing, resource monitoring and management, SG, and optimization of communication networks and open networking.



Alberto Leon-Garcia (F'99) received the B.S., M.S., and Ph.D. degrees in electrical engineering from the University of Southern California, Los Angeles, CA, USA, in 1973, 1974, and 1976, respectively.

From 1999 to 2002, he was the Founder and CTO of AcceLight Networks, Ottawa, ON, Canada, which developed an all-optical fabric multiterabit switch. Currently, he is a Professor in the Electrical and Computer Engineering Department, University of Toronto, ON, Canada.

His current research interests include application-oriented networking and autonomic resources management with a focus on enabling pervasive smart infrastructure.

Prof. Leon-Garcia is the author of the leading textbooks *Probability and Random Processes for Electrical Engineering* (Reading, MA, USA: Addison-Wesley, 1989) and *Communication Networks: Fundamental Concepts and Key Architecture* (New York, NY, USA: McGraw-Hill, 2006). He is a Fellow of the Engineering Institute of Canada. He received the 2006 Thomas Eadie Medal from the Royal Society of Canada and the 2010 IEEE Canada A. G. L. McNaughton Gold Medal for his contributions to the area of communications.

867
868
869
870
871
872
873
874
875
876
877
878
879
880
881
882
883
884
885
886
887
888
889

Queries

- | | |
|---|-------------------|
| Q1. Author: Please provide expansion of acronym "ToU." | 890 |
| Q2. Author: Please provide the subject in which the author "Mohammad Hossein Yaghmaee Moghaddam" received the B.Sc. degree. | 891
892
893 |

IEEE Proof

Autonomous Two-Tier Cloud-Based Demand Side Management Approach with Microgrid

Mohammad Hossein Yaghmaee Moghaddam, *Senior Member, IEEE*,
Morteza Moghaddassian, *Student Member, IEEE*, and Alberto Leon-Garcia, *Fellow Member, IEEE*

Abstract—Demand side management (DSM) is an important application of the future smart grid. DSM programs allow consumers to participate in the operation of the electric grid by reducing or shifting their electricity usage during peak periods. Therefore, in this paper, we propose a two-tier cloud-based DSM to control the residential load of customers equipped with local power generation and storage facilities as auxiliary sources of energy. We consider a power system consisting of multiple regions and equipped with a number of microgrids. In each region, an edge cloud is utilized to find the optimal power consumption schedule for customer appliances in that region. We propose a two-level optimization algorithm with a linear multilevel cost function. At the edge cloud, the power consumption level of local storage and the amount of power being demanded from both local storage facilities and power grid are scheduled by using a bi-level optimization approach. The core cloud then gathers information of the total demand from consumers in different Regions and finds the optimal power consumption schedule for each microgrid in the power system. Simulation results show that the proposed model reduces consumption cost for the customers and improves the power grid in terms of peak load and peak-to-average load ratio.

Index Terms—Cloud computing, demand side management (DSM), home energy management systems (HEMS), optimization, power consumption scheduling.

I. INTRODUCTION

THE smart grid (SG) uses two-way communications to gather the information from different parts of a power network. This information is used to monitor and control the generation, transmission, and distribution equipment. Information and communications technology (ICT) is the foundation of many applications in the SG. By utilizing ICT capabilities, the SG improves the efficiency, reliability, and sustainability of the power grid, and it delivers many benefits including efficient transmission of electricity, quick restoration of electricity

Manuscript received May 26, 2016; revised September 12, 2016; accepted October 9, 2016. Paper no. TII-16-0481. (Corresponding author: M. H. Y. Moghaddam.)

M. H. Y. Moghaddam is with the Department of Computer Engineering, Ferdowsi University of Mashhad, Mashhad 91779, Iran and also with the Department of Electrical and Computer Engineering, University of Toronto, Toronto M5S 3G4, ON, Canada (e-mail: hyaghmae@um.ac.ir).

M. Moghaddassian and A. Leon-Garcia are with the Department of Electrical and Computer Engineering, University of Toronto, Toronto M5S 3G4, ON, Canada (e-mail: m.moghaddassian@mail.utoronto.ca; alberto.leongarcia@utoronto.ca).

Color versions of one or more of the figures in this paper are available online at <http://ieeexplore.ieee.org>.

Digital Object Identifier 10.1109/TII.2016.2619070

after power disturbances, reduced operations and management costs for utilities, low power costs for consumers, reduced peak demand, increased integration of large-scale renewable energy systems, better integration of customer-owner power generation systems, and improved security.

Demand response (DR), which is one of most important applications of the SG, can be used in the future smart cities to inform consumers about their energy usage and costs. Smart consumers can make decisions autonomously about how and when to use electricity. By developing the Internet of Things (IoT) technology, it is possible to transfer customer's power consumption information to the cloud and develop a central demand side management (DSM) program to control and schedule the customer's appliances centrally. Without utilizing the SG applications, it is not possible to develop the smart cities. As described in [1], the IoT can be used to furnish intelligent management of energy distribution and consumption in heterogeneous circumstances. By leveraging the IoT-based appliances, the smart customers can send their optimal schedule to the utility companies. In the recent years, by the growth of IoT and digital technologies, smart cities have been becoming smarter than before.

In this paper, we propose a cloud-based DSM program that schedules the power consumption by customers in different regions and in microgrids so that both customer and utility company costs are optimized. There is a noticeable confluence between our proposed approach and the smart cities and IoTs, and that is the concept of service layer abstraction. More clearly, the proposed model can be implemented as an energy management component of the smart city that provides consumer electricity consumption management as a service. This concept defines many benefits including modularity in designing smart cities components and reducing the time and effort to extend the smart city services. Furthermore, it is designed to run on commodity hardware on a cloud computing platform, where the aggregation of hardware resources provides more power than any individual computing box. It can be considered as a data-driven model that can be further adjusted for any other utility management services. Cloud-based nature of the proposed model reduces the cost of computation that makes it easier for our future smart cities to deploy such services in future smart cities.

The cloud-based DSM utilizes the processing and storage resources of two-tier cloud computing consisting of the "Smart Edge" and the "Core cloud," to develop an optimal DSM. In our architecture, customers are classified into different regions. Each region is controlled by a "Smart Edge" cloud to provide cloud computing resources at the edge of the network precisely to meet low latency requirements as well as to

89 reduce the volume of traffic that needs to traverse the network
90 backbone. The core cloud performs a central optimization
91 at the multiregion level. At the customer side, consumption
92 information and local generation data are forwarded to an edge
93 cloud for the region. The edge cloud runs an optimization
94 process to find the optimal power consumption schedule for
95 both user appliances and local storage. After the edge cloud
96 obtains the optimal schedule for both appliances and local
97 storage devices, the total optimal load schedule of each region is
98 calculated and forwarded to the core cloud. The core cloud has
99 the load information for each region, and it also knows the
100 total stored energy in each microgrid. It can therefore perform
101 a centralized optimization to schedule the resource usage in the
102 microgrids so that the total multiregion cost is minimized. Our
103 main motivations for proposing a cloud-based DSM program are
104 as follows.

105 1) The single point of failure and the distributed denial-
106 of-service (DDoS) attacks from compromised nodes are
107 some significant concerns in the DR programs that are
108 based on master-slave architecture where the utility is
109 the master and customers are slaves. Although there are
110 solutions that are totally auto-reconfigurable and fault-
111 tolerant [2], but DDoS attack is still a big concern in
112 these approaches. By utilizing the cloud computing, the
113 proposed DSM model can decrease the negative effects
114 of DDoS attacks. The elastic nature of cloud comput-
115 ing allows it to provide the required communication and
116 computation resources, dynamically as needed especially
117 when a DOS attack happens. As the proposed DSM is
118 based on two-tier cloud computing, it can leverage the
119 existing defense method to prevent possible DDoS at-
120 tacks by rapidly provisioning resources when any attack
121 happens. The cloud-based DSM model can utilize some
122 popular methods against the DDoS attacks.

123 2) Current energy management systems that are used by
124 utilities to perform the DR programs suffer from lim-
125 ited memory and storage, especially, when the number
126 of customers is increased. By increasing the number of
127 customers in the system, to store the customer's data
128 and run the optimization process more computation and
129 storage resources are needed. In the cloud-based DSM
130 solution, as the optimization program is run at the cloud
131 server the memory and processing resources are always
132 available. When we need more resources (due to increase
133 in the number of customers or the size of optimization
134 problem), the cloud server can easily use some techniques
135 such as autoscaling to scale up the virtual machine and in-
136 crease its resources. Increasing the number of customers
137 in the optimization problem also increases the execution
138 time. So, we partition the problem into two parts edge
139 and core clouds which provides high scalability and fast
140 response time. Together these "edge clouds" and "core
141 clouds" create a multitier computing cloud. The motiva-
142 tions for these edge clouds certainly apply to SGs, and so
143 we explore the DSM in this multitier context. We utilize
144 the high processing and storage capabilities of multitier
145 cloud computing to run central optimization problems.

3) In the decentralized DSM, the optimization problem is
146 solved by the Energy Consumption Scheduler (ECS),
147 which is usually placed in the Home Energy Management
148 System (HEMS), or smart meter, which has limited com-
149 putational and capacity powers. In the distributed DSM
150 approaches, many iterations should be performed to find
151 the optimum solution. For example, for the distributed
152 DSM program given in [3] and for a power network with
153 100 users, when the channel bit error rate is 0.01 al-
154 most 10^6 update messages are exchanged to converge to
155 the optimal solution. In contrast, in the proposed cloud-
156 based DSM, all necessary calculations are performed at
157 the cloud servers provided by the utility companies. It
158 means that the users do not need to spend money to buy
159 sophisticated HEMS. They just need to participate in the
160 cloud-based energy efficient programs provided by the
161 utility companies or third party to optimize their energy
162 consumption.

163 4) In DSM programs based on the game theory (such as [3],
164 [4]), customers are classified in some clusters with dif-
165 ferent members. A local communications network needs
166 to be established between all customers. The assump-
167 tion that the customers have knowledge about their own
168 and the other customers' pay-offs is not practical. Fur-
169 thermore, techniques for solving games by using mixed
170 strategies, particularly for large pay-off matrix, are too
171 complicated. Unlike the decentralized DSM models, the
172 proposed work is based on the central optimization at the
173 cloud server. It means that the customers do not need to
174 communicate and cooperate together to find the optimal
175 solution. Entire operation is performed centrally at the
176 cloud server. We just need to collect the power consump-
177 tion information from all the customers and then run the
178 optimization problem. As the central server has a global
179 view of the power system, achieving an optimized solu-
180 tion is more feasible than the decentralized approaches
181 that are based on the local information.

182 5) When the power consumption scheduling is performed in
183 the distributed fashion, security is a big challenge. In the
184 distributed DSM, customers broadcast their local optimal
185 solutions. It has been proven that data broadcasting is not
186 secure. The hackers may access the ECS data, change
187 the users' consumption and scheduling information, and
188 broadcast fake data to other users in the same cluster.
189 Cloud computing offers a deployment architecture, with
190 the ability to address vulnerabilities recognized in the
191 traditional information security. Cloud-based DSM can be
192 more secure than the decentralized DSM by using some
193 approaches such as multifactor authentication, security
194 patching, physical security, and security certifications.

195 6) Current grid technology suffers from peak loads that
196 arise from a drop in the supply or an increase in the
197 demand. It also limits the DR to static strategies, such
198 as time of use pricing and day-ahead notification based
199 on historical averages. In the proposed model, we
200 consider the photovoltaic (PV) based microgrid as an
201 auxiliary source of energy in our model and optimize it
202

so that the customer's cost could be minimized. Since microgrids are independent of the power grid, they can continue operating while the main grid is down. They can function as a grid resource for faster system response and recovery. Also, in the proposed model, the use of local sources of energy to serve local loads helps reduce energy losses in the transmission and distribution.

The rest of this paper is organized as follows. Section II, presents the literature review and background. In Section III, we explain the proposed model in detail. Section IV shows the simulation results that confirm the superior performance of the proposed model. Finally, Section IV concludes the paper.

II. LITERATURE REVIEW AND BACKGROUND

During past few years lot of research work has been devoted to DSM programs. There is now a rich literature on using optimization techniques and game theory to manage the demand at the customer side by minimizing the cost of power generation or maximizing the customers' utility [3]–[9]. Phase change materials (PCM) play a significant role in the future of buildings. PCM can be used for thermal energy storage system because simply it would be possible to include it into building components such as walls. In [10] by considering price-based and incentive-based DR programs, an optimized HEMS that employs the PCM for decreasing the residential demand and cost has been designed. As investigated in [10], when PCM is combined with the HEMS, the battery usage is reduced as compared to the case without PCM. In case of using PCM, most of the battery energy is utilized at the peak hour where the energy price is high. Dusparic *et al.* [11] define a decentralized DR approach that can be used to minimize the amount of residential power consumption, by maximizing the utilization of the generated power from wind energy resources. For a power system consisting of electric vehicles and wind renewable energy generators, the distributed W-Learning algorithm has been utilized. Each customer device is controlled by an intelligent agent that learns how to meet multiple goals and objectives. However, this approach suffers from some problems. First, distributed DR is based on the local objective function so finding the global solution especially when there are a lot of customers in the system is not possible. Second, cloud-based demand response (CDR) can utilize the autoscaling capabilities of cloud computing to adjust the necessary computation resources dynamically and provide more scalability and flexibility. The work in [12] for the customer homes with the time of use energy pricing, proposes two different DR and scheduling approaches including centralized and decentralized. In the decentralized mode, a microprocessor with a stand-alone algorithm is added to the smart plug (SP), to schedule the SPs optimally. However, adding microprocessor and related software to the SPs make them expensive for the customers. In the centralized approach, a central controller located at the HEMS, gathers the necessary information from the SPs to optimally schedule the SPs inside the home. However, this model does not consider the use of small power generation facilities and is not as broad as our model. Siano and Sarno [13] present a DR program considering the distribution locational

marginal price (D-LMP) energy market. It is supposed that customers can receive D-LMP price signal through the home gateway. The customers can join the real-time DR program by installing some specific equipment. The proposed optimization tries to maximize the benefit of the consumers and minimize the production cost of the producer. However, it just considers the fixed and shiftable loads and does not support the optimal scheduling of the local PV and microgrid in the model.

Recently, cloud computing has received attention for SG applications [14]–[16]. Most SG applications need reliable and efficient communications. This can be met by utilizing the cloud computing based on the software-defined infrastructure [17]. As investigated in [16] and [18], cloud computing brings some opportunities for SG applications. Flexible resources and services shared in the network, parallel processing, and omnipresent access are some features of cloud computing that are desirable for SG applications. Kim *et al.* [19] present the architecture of CDR which outperforms the previous work in terms of convergence speed while keeping the same messaging overhead.

III. PROPOSED MODEL

In this section, we present our proposed power system model and the cost function.

A. System Model

We assume that there are R different regions in the system. In each region r , there are m_r , $r \in \{1, \dots, R\}$ customers that are connected to the grid and consume energy. There are M distinct microgrids in the system. Each microgrid consists of distributed generation (DG) and distributed storage units. Without the loss of generality, we consider PV energy generation in each microgrid. We consider a two-tier cloud consisting of edge and core clouds. The edge cloud gathers the consumption (and also generation) information from all customers in each region and finds the optimal power consumption schedule for the customers so that the total energy consumption cost is minimized. Using existing data networks, the optimal consumption schedule is transferred to the HEMS. After all the edge clouds have calculated the optimal power consumption schedule of all customers in all regions, the total scheduled load information is transferred to the core cloud. The core cloud computes the total scheduled load gathered from the all edge clouds. Based on the total hourly load in the system, the core cloud schedules the optimal power consumption in each microgrid so that the peak-to-average ration (PAR) is decreased.

B. Power Consumers

We define three different types of power consumers.

- 1) *Type 0*: These are traditional power consumers. Type 0 consumers neither have local generation and storage nor the HEMS. It is not possible to schedule the power consumption for these consumers. These consumers do not require a data connection to the cloud. We consider these consumers as a variable hourly load in the power system that is not shiftable.

310 2) *Type 1*: These consumers have the HEMS, and two types
 311 of appliances, shiftable and nonshiftable. These con-
 312 sumers have a data connection to the cloud by using
 313 the HEMS. In order to minimize the power consumption
 314 cost and also reduce the PAR, the power consumption of
 315 shiftable appliances is scheduled.

316 3) *Type 2*: These are sophisticated consumers that are
 317 equipped with local generation and storage as well as the
 318 HEMS. When the main power grid is disconnected, which
 319 usually happens due to outages and the other source of
 320 blackout, the customers can use the local energy gen-
 321 eration and storage systems. These consumers generate
 322 part of their required energy by using PV systems. We
 323 assume that the generated power is stored in the local
 324 storage (battery) and is consumed by local appliances.

325 Let m_r^0 , m_r^1 , and m_r^2 denote the number of Type 0, Type 1, and
 326 Type 2 consumers, respectively, in region r , $r \in \{1, \dots, R\}$. As
 327 Type 0 consumers are not controllable, in the rest of this paper
 328 we consider just Type 1 and Type 2 consumers. For any cus-
 329 tomer n in region r , $n \in \{1, \dots, m_r\}$, $r \in \{1, \dots, R\}$, let $A_{r,n}$
 330 denote the set of appliances of this customer. We define $X_{r,n,a}$
 331 as the energy consumption scheduling vector, where $a \in A_{r,n}$
 332 denotes the appliance number and H is the scheduling horizon
 333 that indicates the number of hours ahead which are taken into
 334 account for decision making in energy consumption scheduling.
 335 We define $X_{r,n}$ vector as energy consumption scheduling vector
 336 for all appliances of customer n in region r . For Type 2 con-
 337 sumers, we define $P_{r,n} = \{p_{r,n}^1, p_{r,n}^2, \dots, p_{r,n}^h, \dots, p_{r,n}^H\}$, as
 338 the total power generation vector where $p_{r,n}^h$ denotes the amount
 339 of energy generated by the local PV system of customer n in
 340 region r at time h . In the next section, we will describe the
 341 proposed local generation model in detail.

342 The state of the charge (SOC) is one of the most important
 343 parameters for batteries that is defined as the ratio of its cur-
 344 rent capacity to the nominal capacity. The nominal capacity
 345 represents the maximum amount of charge that can be stored
 346 in the battery. The Coulomb counting method has been applied
 347 in order to estimate the SOC [20]. Suppose $\text{SOC}_{r,n}^h$ and $B_{r,n}^F$
 348 represent the SOC and the nominal battery capacity, respec-
 349 tively, of customer n in region r at time h . The current value of
 350 SOC ($\text{SOC}_{r,n}^h$) based on its previous value ($\text{SOC}_{r,n}^{h-1}$) and the
 351 charging/discharging current $I_b(t)$ is estimated as

$$\text{SOC}_{r,n}^h = \text{SOC}_{r,n}^{h-1} + \frac{I_b(t)}{B_{r,n}^F} \Delta t. \quad (1)$$

352 We define $B_{r,n} = \{b_{r,n}^1, b_{r,n}^2, \dots, b_{r,n}^h, \dots, b_{r,n}^H\}$, as the bat-
 353 tery state vector where $b_{r,n}^h$ denotes the amount of energy stored
 354 in the battery of customer n in region r at time h . Due to the lim-
 355 ited capacity of local storages, the following condition should
 356 be satisfied:

$$0 \leq b_{r,n}^h \leq B_{r,n}^F. \quad (2)$$

357 The value of $b_{r,n}^h$ is obtained by the following equation:

$$b_{r,n}^h = \text{SOC}_{r,n}^h \cdot B_{r,n}^F. \quad (3)$$

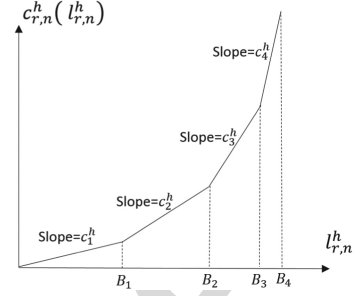


Fig. 1. Proposed N levels IBR pricing model.

358 Suppose $g_{r,n}^h$ and $y_{r,n}^h$ denote the amount of energy generation 358
 359 and consumption of Type 2 customer n in region r at time h . 359
 360 We assume that the customer consumes its available power in local 360
 361 storage first and then demands power from the power grid, if 361
 362 needed. We define $G_{r,n} = \{g_{r,n}^1, g_{r,n}^2, \dots, g_{r,n}^h, \dots, g_{r,n}^H\}$ and 362
 363 $Y_{r,n} = \{y_{r,n}^1, y_{r,n}^2, \dots, y_{r,n}^h, \dots, y_{r,n}^H\}$ as the power generation 363
 364 and consumption vector from the PV system, respectively. As 364
 365 the battery is charged by the solar energy ($g_{r,n}^h$) and is dis- 365
 366 charged by the local consumption ($y_{r,n}^h$), by combining (3) in 366
 367 (1) we have 367

$$b_{r,n}^h = b_{r,n}^{h-1} + g_{r,n}^h - y_{r,n}^h, \quad h = 2, \dots, H. \quad (4)$$

368 We define $l_{r,n}^h = X_{r,n}^h - y_{r,n}^h$ as the total household 368
 369 energy consumption at each upcoming hour h . 369

C. Consumer Price Model 370

371 The proposed price model is designed by combining the 371
 372 real-time pricing (RTP) and inclining or increasing block rates 372
 373 (IBR) and considering N different blocks shown in Fig. 1. Our 373
 374 main objective of proposing this pricing model is to charge 374
 375 a higher rate per kilowatt-hour (kWh) at higher levels of en- 375
 376 ergy usage and a lower rate at lower usage levels. The total 376
 377 cost of the customers who consume low energy (lower blocks) 377
 378 is less than those who consume more energy (higher blocks). 378
 379 The first block of B_1 kWh would cost c_1^h per kWh, the sec- 379
 380 ond block of B_2 kWh would cost c_2^h per kWh, and so on. 380
 381 Note that $c_i^h > c_{i-1}^h > 0$, $i \in \{2, \dots, N\}$, which means that 381
 382 the proposed pricing model charges a higher rate for each incre- 382
 383 mental block of consumption. To support the RTP, the price 383
 384 factors c_i^h are time dependent and may be changed hourly. For 384
 385 example suppose $N = 7$ and $B_i = i$ kWh. Based on the prop- 385
 386 osed pricing model the total power consumption cost for a 386
 387 customer with 6.5 kWh power consumption is computed as 387
 388 $(\sum_{i=1}^6 c_i^h + 0.5 c_7^h)$. Unlike the ToU and flat pricing, the intro- 388
 389 duction of IBR leads to energy savings. Another advantage 389
 390 of the proposed pricing is that it is straightforward and easy 390
 391 to understand by households. In the proposed pricing model, 391
 392 the cost of each block can be changed in real time. For each 392
 393 customer n in region r at time h , the power consumption cost 393
 394 $c_{r,n}^h(l_{r,n}^h)$ is calculated as follows (5) shown at the bottom of the 394
 395 next page. 395

396 It can be seen that the proposed cost function is increasing
397 and strictly convex. It means that

$$c_{r,n}^h(\hat{l}_{r,n}^h) < c_{r,n}^h(\tilde{l}_{r,n}^h), \quad \forall \hat{l}_{r,n}^h < \tilde{l}_{r,n}^h. \quad (6)$$

$$c_{r,n}^h(\varepsilon \hat{l}_{r,n}^h + (1 - \varepsilon) \tilde{l}_{r,n}^h) < \varepsilon c_{r,n}^h(\hat{l}_{r,n}^h) + (1 - \varepsilon) c_{r,n}^h(\tilde{l}_{r,n}^h). \quad (7)$$

398 As the proposed power system model is based on the hier-
399 archical model that consists of different regions, we can define
400 different price functions for different regions. This is because
401 each region is responsible for the power consumption optimiza-
402 tion of its customers. So, the proposed region-based optimiza-
403 tion allows us to take the geolocation of customers into account,
404 which helps us to prevent the possible congestion and peak
405 loading within particular regions. For instance, when a power
406 overload occurs at a particular region, the utilities may increase
407 the power price at that particular time at the specific region.
408 Thus, customers are encouraged to decrease their power con-
409 sumption or shift it to the nonpeak hours.

410 D. Distributed Power Generation Model

411 We suppose that PV systems are used for DG by Type 2
412 consumers and in microgrids. It has been proven that the total
413 energy generation by PV systems depends on parameters such
414 as temperature, total solar panel area, solar panel yield, and
415 performance of the installation including all losses (inverter
416 losses, temperature losses, dc and ac cables losses, shadings,
417 losses due to weak radiation, and losses due to dust and snow).

418 Previous studies [21]–[24] show that the power output of a
419 PV module depend linearly on the operating temperature. The
420 electrical performance is primarily influenced by the type of
421 PV used. A typical PV module converts 6–20% of the incident
422 solar radiation into electricity, depending upon the type of solar
423 cells and climatic conditions. The rest of the incident solar ra-
424 diation is converted into heat, which significantly increases the
425 temperature of the PV module and reduces the PV efficiency
426 of the module. To consider the effect of temperature in our PV
427 generation model, based on works given in [21] and [24], we
428 propose the following equation:

$$G_{pv} = A \cdot \mu \cdot \vartheta \cdot \tau_s \cdot (1 + \alpha (T_m - 25)) \quad (8)$$

429 where G_{pv} is the total annually energy generation (kWh), A
430 is the total solar panel area (m^2), μ is the solar panel yield
431 (default value %15), ϑ is the annual average irradiation on
432 tilted panels, which is changed regionally (between 500 and
433 2500 kWh/m².an), τ_s is the performance ratio and coefficient
434 for losses (default value %75), T_m is the temperature (in centi-
435 grade), and α is the temperature coefficient for power of the PV
436 module, which is $-0.20\%/^\circ\text{C}$.

Suppose $G_{h,d}^0$ represents the solar cell energy generation at
each hour h in day d when the sky is clear. When the sky is
cloudy, the energy generation is a portion of $G_{h,d}^0$ depending on
the cloud coverage. It is clear that the cloud coverage is related
to the time and the day of year. As it has been investigated
in [25], at each hour h in day d , the amount of solar energy
generation $G_{h,d}^F$ is calculated as follows:

$$G_{h,d}^F = K \cdot f(d) \cdot g(h) \cdot (1 - 0.75F_{h,d}^3) \quad (9)$$

where $F_{h,d}$ is the fraction of sky cloud cover on a scale from 0
(no clouds) to 1 (complete coverage) at time h of day d , K is a
normalization constant, and $f(d)$ and $g(h)$ are two functions
that indicate how much of the sun's power can be captured
in each hour for a particular day of the year. $f(d)$ is given as
follows [26]:

$$f(d) = \frac{\sin(90 - \varphi + \phi(d))}{\sin(90 - \varphi + \phi(d) + \theta)} \quad (10)$$

where φ and θ are latitude and the tilt angle of the module
measured from the horizontal, respectively. $\phi(d)$ is declination
angle calculated as [26]

$$\phi(d) = 23.45^\circ \cdot \sin\left(\frac{360}{365}(284 + d)\right). \quad (11)$$

The tilt angle has a major impact on the solar radiation in-
cident on a surface. For a fixed tilt angle, the maximum power
over the course of a year is obtained when the tilt angle is equal
to the latitude of the location ($\varphi = \theta$). We propose the following
Gaussian function for $g(h)$:

$$g(h) = e^{-\frac{(h-h_0)^2}{2\sigma^2}}, \quad h_0 = (t_{\text{sunset}} + t_{\text{sunrise}})/2 \quad (12)$$

where h_0 and σ^2 are the center and the variance of the Gaussian
function, respectively. t_{sunset} and t_{sunrise} are the sunset and
sunrise time, respectively. By substituting (10)–(12) into (9),
 $G_{h,d}^F$ is obtained as follows:

$$G_{h,d}^F = K \frac{\sin(90 - \varphi + \phi(d))}{\sin(90 - \varphi + \phi(d) + \theta)} e^{-\frac{(h-h_0)^2}{2\sigma^2}} (1 - 0.75F_{h,d}^3). \quad (13)$$

As the total energy generation during all hours of all days in
a year should be equal to the annual energy generation, the
constant parameter K is obtained as follows:

$$K = \frac{G_{pv}}{\sum_{d=1}^{365} \sum_{h=1}^{24} \frac{\sin(90 - \varphi + \phi(d))}{\sin(90 - \varphi + \phi(d) + \theta)} e^{-\frac{(h-h_0)^2}{2\sigma^2}} (1 - 0.75F_{h,d}^3)}. \quad (14)$$

To investigate the accuracy of the PV generation model, we
compare the output of the PV generation model with that of the
3.15 kW PV system located in West Hobart, TAS, Australia [27],
and for date July 1, 2016. The real PV system generations were

$$c_{r,n}^h(l_{r,n}^h) = \begin{cases} c_1^h \cdot l_{r,n}^h & \text{if } B_0 = 0 \leq l_{r,n}^h \leq B_1 \\ \sum_{i=1}^{j-1} c_i^h \cdot (B_i - B_{i-1}) + c_j^h \cdot (l_{r,n}^h - B_{j-1}), \quad j = 2, \dots, N-1 & \text{if } B_{j-1} < l_{r,n}^h \leq B_j \\ \sum_{i=1}^{N-1} c_i^h \cdot (B_i - B_{i-1}) + c_N^h \cdot (l_{r,n}^h - B_{N-1}) & \text{if } B_{N-1} < l_{r,n}^h \end{cases} \quad (5)$$

TABLE I
COMPARISON OF THE PV GENERATION MODEL WITH REAL DATA

Hour	8	9	10	11	12	13	14	15	16	17
Temperature	5.4	7.7	9.3	11.1	12	12.7	11.9	11.8	11.4	11.3
Real data	0.0	0.4	0.83	0.74	0.97	0.98	0.48	0.16	0.12	0.009
PV model	0.07	0.2	0.44	0.73	0.94	0.94	0.71	0.42	0.19	0.07

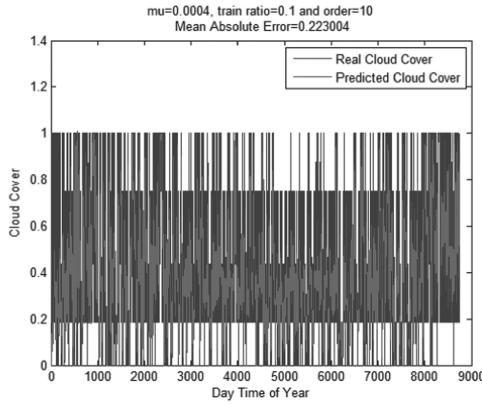


Fig. 2. Cloud coverage prediction efficiency (Toronto region, Jan. 1, 2015–Jan. 1, 2016).

469 measured and compared with the output of the proposed model.
470 The sunrise time, sunset time, and altitude of West Hobart, TAS,
471 were set to 8 A.M., 17 P.M., and 24 °S, respectively. The results
472 given in Table I, confirm that the proposed PV model has almost
473 0.13 mean absolute error.

474 E. Cloud Cover Prediction

475 Since the proposed model is based on a day-ahead optimization,
476 we have to know the amount of energy generation of the
477 Type 2 consumers and the microgrids in each hour of the next
478 day. For this purpose, we use (13), to evaluate the amount of
479 energy generation of PV systems for the next day. We also need
480 to estimate the cloud coverage $F_{h,d}$. The normalized least mean
481 square (NLMS) [28] predictor is the one providing the best
482 tradeoff between complexity, accuracy, and responsiveness. We
483 used the historical cloud coverage data given in [29] to tune the
484 filter parameters. The NLMS predictor needs the configuration
485 of two parameters: the order p and the step size μ . These param-
486 eters should be set correctly so that the best performance with
487 minimum error is obtained. In the case of the μ , it is relevant
488 to note that one of the main advantage of using NLMS is that
489 it is less sensitive to the step size with respect to other linear
490 predictor. In Fig. 2, at each hour of a day for the period of Jan. 1,
491 2015–Jan. 1, 2016 and for the Toronto city, the real cloud cover
492 and its prediction is plotted versus each hour of the day in the
493 year (totally $24 * 365 = 8760$ samples).

494 F. Edge Cloud Cost Optimization

495 As mentioned earlier, in each region there is an edge cloud
496 that gathers all the customers' consumption information to op-
497 timize the power consumption schedule. The optimal schedule
498 is obtained by the use of two-level optimization approach with
499 the predefined cost function as follows.

Level 1 optimization (for both Type 1 and Type 2 consumers): 500
In this stage the consumption pattern of all customer's shiftable 501
appliances in each region is scheduled by using the following 502
optimization problem: 503

$$\text{minimize } \sum_{h=1}^H c_{r,n}^h \left(\sum_{n=1}^{m_r} \sum_{a \in A_{r,n}} x_{r,n,a}^h \right)$$

Subject to

$$\alpha_a \leq x_{r,n,a}^h \leq \beta_a$$

$$\sum_{h=1}^H x_{r,n,a}^h = E_{r,n,a}$$

$$\gamma_{r,n}^{\min} \leq \sum_{a \in A_{r,n}} x_{r,n,a}^h \leq \gamma_{r,n}^{\max}$$

$$\text{Output : } x_{r,n,a}^* \quad (15)$$

where $E_{r,n,a}$ denotes the total energy needed for the operation 504
of appliance a of customer n in region r . α_a and β_a are the 505
beginning and end of a time interval, respectively, in which the 506
energy consumption for appliance a is valid, γ_a^{\min} and γ_a^{\max} 507
are the minimum and maximum power levels denoted of home 508
appliances. After optimization and thus rescheduling of shiftable 509
appliances, for each shiftable appliance a of customer n in 510
region r , the optimized energy consumption scheduling vector 511
 $X_{r,n,a}^*$ is obtained. By considering the nonshiftable and shiftable 512
appliances the optimal ECS vector $X_{r,n}^*$ for all appliances of 513
customer n in region r is obtained. 514

Level 2 optimization (only for Type 2 consumers): Type 2 515
consumers generate part of their energy consumption by using 516
the local generation such as the PV system. This energy is 517
stored in the batteries and consumed at the proper time. The 518
question is that to minimize the energy cost, what is the best 519
time for consuming this stored energy? To answer this question, 520
the following optimization problem is defined: 521

$$\text{minimize } \sum_{h=1}^H \sum_{n=1}^{m_r} c_{r,n}^h \left(x_{r,n}^{*h} - y_{r,n}^h \right).$$

Subject to:

$$\sum_{a \in A_{r,n}} x_{r,n,a}^{*h} \leq x_{r,n}^{*h},$$

$$\sum_{h=1}^H x_{r,n}^{*h} = \sum_{a \in A_{r,n}} E_{r,n,a}$$

$$0 \leq b_{r,n}^h \leq g_{r,n}^h$$

$$\sum_{h=1}^H g_{r,n}^h = \sum_{h=1}^H y_{r,n}^h$$

$$y_{r,n}^1 \leq b_{r,n}^1 \rightarrow b_{r,n}^1 = g_{r,n}^1$$

$$y_{r,n}^i \leq b_{r,n}^i \rightarrow b_{r,n}^i = b_{r,n}^{i-1} + g_{r,n}^i - y_{r,n}^{i-1}, i = 2, \dots, H$$

$$\text{Output : } y_{r,n}^* \quad (16)$$

Algorithm 1: Executed by each smart meter of Type 1 and Type 2 consumers.

- 1: **Randomly** initialize $x_{r,n,a}$ for Type 1 consumers and $G_{r,n}$, $B_{r,n}$ and $Y_{r,n}$ vectors for Type 2 consumers
 - 2: **Repeat**
 - 3: **At** random time instances **Do**
 - 4: **Send** vectors $x_{r,n,a}$ for Type 1 and Type 2 consumers and $G_{r,n}$, $B_{r,n}$ and $Y_{r,n}$ vectors for Type 2 consumers to the regional edge cloud server
 - 5: **if** changes happen to the vectors as a result of re/scheduling **Then**
 - 6: **Receive** optimized vectors $x_{r,n,a}^*$ for Type 1 and Type 2 consumers and $Y_{r,n}^*$ just for Type 2 consumers from the regional edge cloud server
 - 7: **Build** vector $X_{r,n}^*$ and **Update** the state of the consumer by building $l_{r,n}^*$ vector
 - 8: **End**
 - 9: **End**
 - 10: **Until** the meter is in service
-

522 where $x_{r,n}^{*h}$ is the optimal energy consumption obtained by the
 523 first optimization and is known. After the above-mentioned op-
 524 timization problem is solved, the optimal power consumption
 525 vector $Y_{r,n}^*$ for local storages is obtained. The consumption load
 526 from the grid is obtained as $l_{r,n}^* = X_{r,n}^* - Y_{r,n}^*$. The optimiza-
 527 tion process in the edge cloud involves two important entities:
 528 smart meter and edge cloud server. The smart meter is involved
 529 for the purpose of power consumption information communi-
 530 cation while the edge cloud server is involved for running the
 531 optimization problem. The smart meter communication with the
 532 edge cloud server is explained in Algorithm 1. This algorithm
 533 is performed by smart meters for just smart consumers (Type 1
 534 and Type 2 consumers).

535 The algorithm for both level 1 and level 2 optimization in the
 536 edge cloud server is explained in detail in Algorithm 2. This
 537 algorithm is performed by each regional edge cloud for its own
 538 Type 1 and Type 2 consumers.

539 G. Core Cloud Cost Optimization

540 After optimization process is completed by each edge cloud,
 541 it sends its total hourly demand load vector to the core
 542 cloud. Each microgrid j , $j \in \{1, 2, \dots, M\}$ also sends vectors
 543 G_j , B_j , and Z_j to the core cloud, which represent the pre-
 544 diction of hourly power generation by microgrid, the remain-
 545 ing energy in the batteries, and the hourly power consumption
 546 level of each microgrid j , $j \in \{1, 2, \dots, M\}$, respectively. Let
 547 $L_h = (L^{th} - z^{th})$, denote the total hourly load in the power
 548 system where L^{th} is the total hourly demand load from all
 549 regions and z^{th} is the total hourly power consumption of all
 550 microgrids in the system are calculated as follows:

$$L^{th} = \sum_{r=1}^R \sum_{n=1}^{m_r} l_{r,n}^{*h} \quad (17)$$

$$z^{th} = \sum_{j=1}^M z_j^h. \quad (18)$$

Algorithm 2: Executed by each edge cloud.

- 1: **Repeat**
 - 2: **For** any Type 1 and Type 2 consumer in the region **Do**
 - 3: **Receive** vectors $x_{r,n,a}$ from any Type 1 and Type 2 consumers and $G_{r,n}$, $B_{r,n}$ and $Y_{r,n}$ vectors from any Type 2 consumers in the region
 - 4: **Solve** linear problem (15) using **IPM** (interior-point method)
 - 5: **if** changes happen to vector $x_{r,n,a}$ **Then**
 - 6: **Send** each vector $x_{r,n,a}^*$ to its corresponding consumers
 - 7: **End**
 - 8: **Solve** linear problem (16) using **IPM** (interior-point method)
 - 9: **if** changes happen to vector $Y_{r,n}$ **Then**
 - 10: **Send** each vector $Y_{r,n}^*$ to its corresponding consumers
 - 11: **End**
 - 12: **Build** $l_{r,n}^*$ vector and **Store** it in the local memory
 - 13: **End**
 - 14: **Build** the vector $l_r^{th} = \sum_{n=1}^{m_r} l_{r,n}^{*h}$ and **Send** it to the core cloud
 - 15: **Until** there is at least on consumer is in service
-

We consider the same linear multilevel cost function from (5) 552
 but with different cost coefficients. The following optimization 553
 problem is defined at the core cloud: 554

$$\text{minimize } \sum_{h=1}^H C_h(L_h) = \sum_{h=1}^H C_h(L^{th} - y^{th}). \quad (19)$$

Note that in the above optimization problem the value for 555
 L^{th} is fixed and is already calculated by edge clouds in the grid. 556
 Therefore, after running the optimization process at the core 557
 cloud, the optimized hourly consumption z^{t*h} from microgrid 558
 storages is obtained. The optimized total hourly load $L_h^* =$ 559
 $L^{th} - z^{t*h}$, which indicates the power consumption level from 560
 power grid, is obtained. The optimization algorithm is explained 561
 in detail in Algorithm 3. This algorithm is performed by the core 562
 cloud for all the entire grid after collecting the supporting data 563
 from all regional edge clouds and microgrids. 564

The operation of whole system is described by the flowchart 565
 given in Fig. 3. 566

567 IV. SIMULATION RESULTS

To compare the performance of the proposed model with that 568
 of the existing work, we consider a central version of work 569
 given in [3] without any Type 2 consumers and microgrids. We 570
 name it reference model. In the simulation model, we consider 571
 a power system that includes 5 regions with 2000 customers in 572
 each region. At each region, the percentage of Type 0, Type 1, 573
 and Type 2 consumers is 50, 30, and 20, respectively. For each 574
 customer we also consider 5–10 appliances with shiftable and 575
 nonshiftable operations. The initial parameters of all appliances 576
 are set by using data given in [30]. We also consider that each 577

Algorithm 3: Executed by the core cloud.

- 1: **Repeat**
- 2: **For** any microgrid $j \in M$ **Do**
- 3: **Receive** vectors G_j, B_j and Z_j
- 4: **End**
- 5: **Build** vector Z^t from the state vectors that have been sent by each microgrid
- 6: **Receive** vector l_r^{th} from each edge cloud server
- 7: **Solve** linear problem (19) using IPM (interior-point method)
- 8: **If** changes happen to the optimization vectors in problem (19) **Then**
- 9: **Build** vectors Z^{t*} and L^* and **Update** the state of the grid
- 10: **End**
- 11: **Until** there is at least one edge cloud server or one microgrid in service

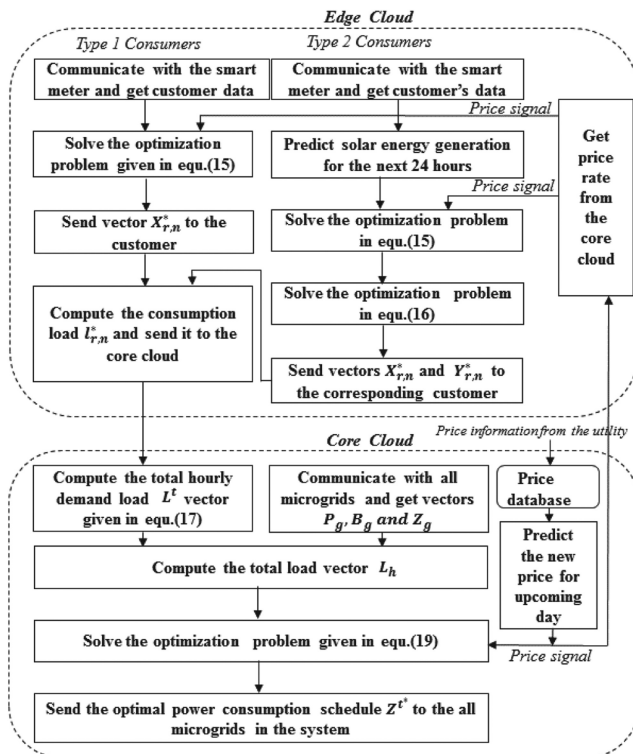


Fig. 3. Flowchart of whole process.

578 Type 2 customer is equipped with the average of 30 m² of
579 photovoltaic cells. Similarly, we consider five microgrids with
580 10 000 m² of solar cells for each. We suppose that the weather
581 temperature for all solar cells is equal to 25 °C. We consider
582 three different power usage intervals (12 A.M.–8 A.M., 8 A.M.–
583 5 P.M., and 5 P.M.–12 A.M.) that correspond to off-peak, mid-
584 peak, and high-peak hours of the day, respectively. The price of
585 each kW power consumption at off-peak, mid-peak, and high-
586 peak hours are supposed to be equal to 0.2, 0.3, and 0.5 cent,
587 respectively. Then for each hour of the day we consider a seven-
588 level pricing system that corresponds to the seven levels of load

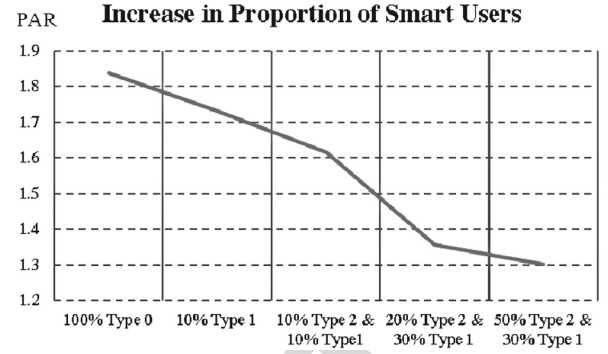


Fig. 4. Effects of the number of smart consumers on the PAR at different combinations of Type 0, Type 1, and Type 2.

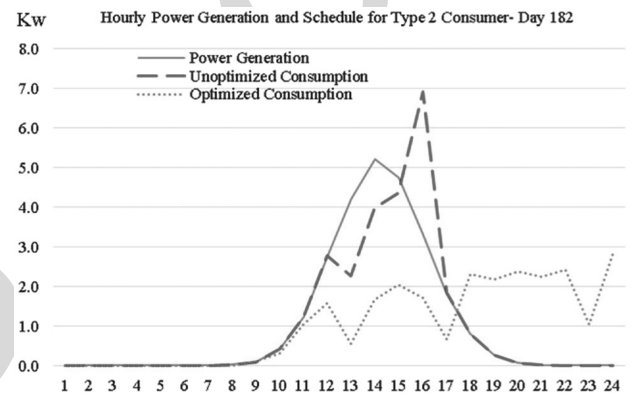


Fig. 5. Hourly power generation and consumption level from local storage facilities, a comparison between unoptimized and optimized approaches.

as defined before by the cost function. We consider the latitude of 589 Toronto, Canada, and set $\varphi = 43^\circ$ N. For the maximum energy 590 observation, we set the tilt angle of the module to the latitude as 591 $\theta = \varphi = 43^\circ$. We consider 31 days simulation interval between 592 Jul. 1 and Jul. 31, 2015 ($d \in [182, 212]$). The cloud coverage 593 data given in [29] are used for training the proposed predictor. 594 We also assume a daily time granularity ($H = 24$). This means 595 that the overall cloud solves the optimization problem for the 596 next 24 h. 597

In the first scenario, we investigate the effects of the number 598 of smart consumers (Types 1 and 2) on the performance of the 599 power system. The results given in Fig. 4 confirm that by 600 increasing the number of smart consumers, the PAR is decreased. 601 For example, when there are 50% Type 2 and 30% Type 1 602 consumers, we can achieve 0.52 decrease in PAR performance 603 comparing with the case that all consumers are Type 0. This 604 results from the higher number of sophisticated participants as 605 well as the higher number of DG resources available. 606

In Fig. 5, for a Type 2 customer and at day 182, the hourly local 607 power generation and usage from the battery (both unoptimized 608 and optimized scenarios) are depicted. It can be seen that almost 609 70% of the power consumption of the total generation of the 610 local PV system is shifted to the peak hours where the price of 611 the power is high. Therefore, the total cost and the amount of 612

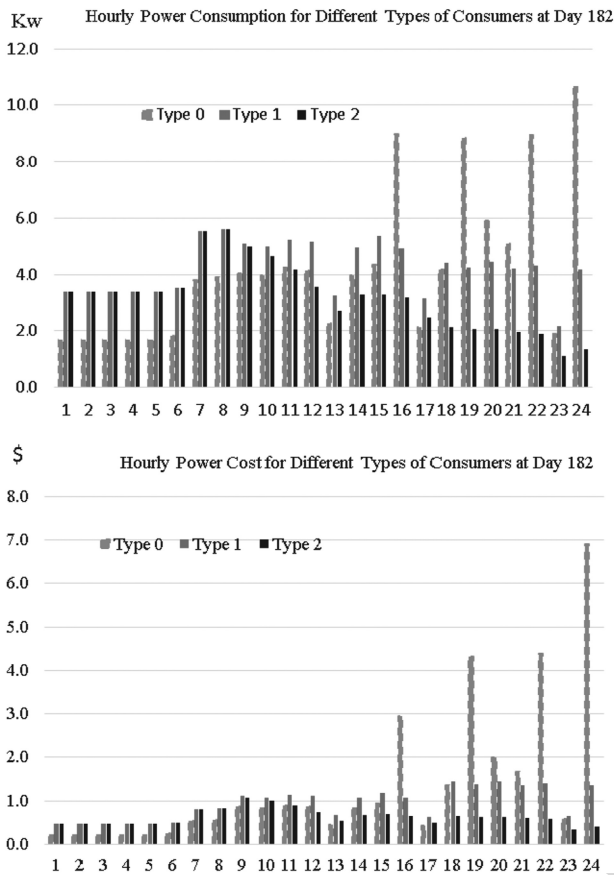


Fig. 6. Effects of smartness level on the hourly power consumption and cost.

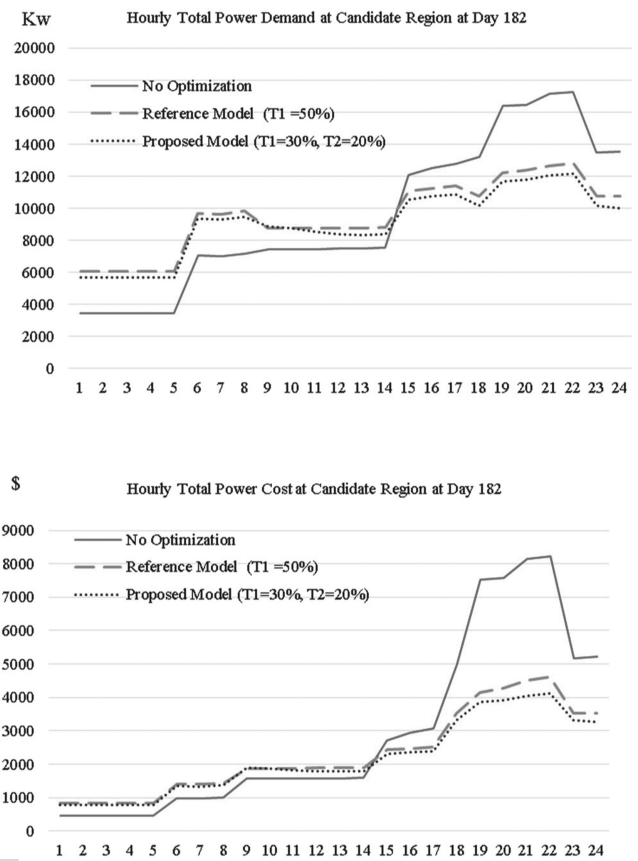


Fig. 7. Hourly power demand level and cost comparison for a candidate region.

613 power consumption from the power grid will be reduced and the
614 grid will experience lower PAR.

615 In Fig. 6, for three candidates Type 0, Type 1, and Type 2 in
616 a given region and at day 182, the hourly power consumption
617 and the power cost are depicted. It can be seen that Type 2
618 consumers save 53.8% and 32.9% in power consumption cost
619 in comparison to Type 0 and Type 1 consumers, respectively.

620 In Fig. 7, for a candidate region with 2000 customers, the
621 hourly regional power demand level and costs are depicted. The
622 figure illustrates a significant improvement from the no opti-
623 mization case and the reference model [3]. It can be seen that
624 in the case of both level 1 and level 2 optimizations (Proposed
625 Model), the total daily cost can be reduced to 26.4% in
626 comparison with the no-optimization case and 6.25% in compar-
627 ison with the reference model [3], with regard to the percentage of
628 Type 1 and Type 2 customers in the region.

629 In Fig. 8, for a power system with five microgrids, and for day
630 182, the amount of power generation in microgrids and power
631 consumption schedule for the microgrid storage are depicted
632 hourly. As the power usage from microgrids is stored in the bat-
633 tery and consumed at peak hours where the price is high, the re-
634 sults confirm that the optimized power consumption scheduling
635 of the microgrid resources save almost \$1.04 per customer daily,
636 in comparison with the unoptimized consumption. This helps
637 to supply part of the customers' demands for electricity without

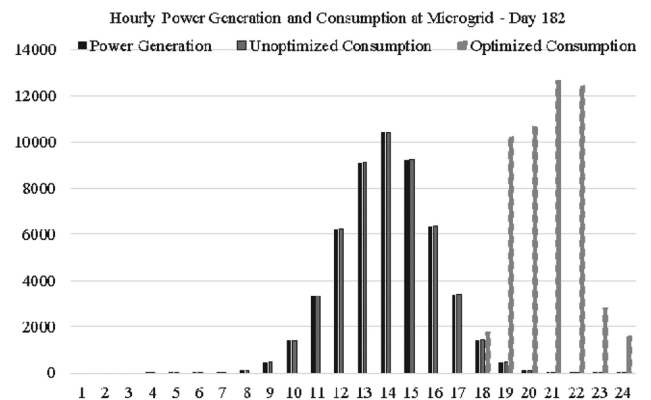


Fig. 8. Effects of the optimization on the hourly power consumption level in microgrids.

638 using grid resources at peak hours. Note that the black bar in
639 Fig. 8 shows how much energy is generated by the microgrids at
640 a particular day whereas the dash bar shows when and how much
641 of this stored energy is consumed by the customers. This con-
642 firms that we store energy in the microgrid's battery during the
643 daytime when the solar energy is high and then consume it at the
644 peak hours when the demand and the energy prices both are high.

645 In Fig. 9, for two different cases of the proposed model (op-
646 timized and unoptimized), the performance of the total grid is
647 evaluated. Optimized refers to the case that microgrid resources

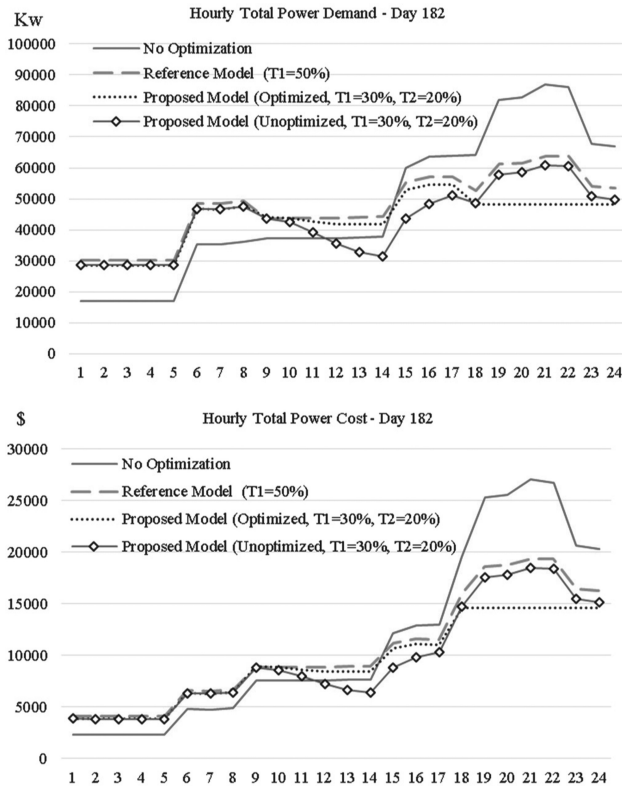


Fig. 9. Hourly grid demand level and costs comparison between no optimization, reference model [3], and the proposed model.

TABLE II
REGIONAL PAR COMPARISON, SHOWING THE IMPACTS OF ADDING MORE TYPE 2 CUSTOMERS

	All Type 0	Reference model [3] (50% Type 1)	Proposed model (30% Type 1, 20% Type2)	Proposed model (30% Type 1, 50% Type2)
Region number 1	1.82	1.35	1.34	1.2853
2	1.83	1.36	1.35	1.2860
3	1.86	1.36	1.35	1.2944
4	1.85	1.35	1.34	1.2880
5	1.83	1.33	1.32	1.2846

are used in the optimal way (after core cloud Algorithm 3 optimization) whereas unoptimized refers to using microgrid resources without any optimal scheduling. The results confirm that using microgrid with optimized scheduling (proposed model, optimized) can significantly improve the grid demand level and cost efficiency. For example, we can save 17.9% and 10.7% in total cost in comparison with no optimization and the reference model [3], respectively. We note that there are five microgrids in the whole grid that are assisted with 10 000 m² of photovoltaic cells, which are capable of generating almost 45 kW of electricity power during a day. By increasing the number of microgrids or the area microgrid solar cells, we can save more in cost and demand.

In Table II, we show that by adding more sophisticated customers (Type 2), the total regional PAR is decreased to a reason-

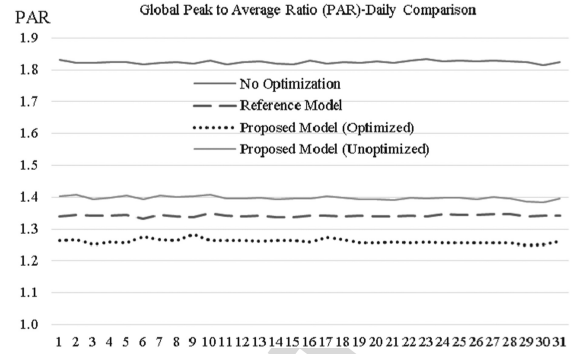


Fig. 10. Investigating the effects of using more sophisticated customers and using microgrids' power generation and storage facilities on the grid PAR.

able degree in comparison with the case of no smart customers (all Type 0). When the percentage of Type 2 consumers is low (20%), the difference between the proposed model and the reference model [3] is negligible. However, it can be seen that as Type 2 consumers place lesser demand on the overall grid, so by increasing the percentage of Type 2 consumers to 50%, the difference between the proposed model and the reference model [3] is increased slightly.

In Fig. 10, for four different approaches (no optimization, reference model [3], and optimized and unoptimized of the proposed model), the total PAR in the grid is plotted at different simulation days (from Jul. 1 to 31). As shown in Fig. 9, optimized refers to the case where microgrid resources are used in optimally (core cloud optimization), and unoptimized refers to use of microgrid resources without any optimal scheduling. It can be seen that using more sophisticated customers and microgrids with optimized power scheduling can significantly reduce the total PAR in the whole grid.

Finally, we investigate the scalability of the proposed model in terms of the convergence time of the optimization process time for different number of customers and regions. The execution time of the whole optimization process (including edge and core clouds) is measured. The proposed optimization is based on three different phases including collecting the information, running the optimization, and transferring the optimal schedule to the customers and microgrids. The optimization processing time directly depends on the performance of the cloud server and the number of customers and regions. When customers are spread in different regions, the required time for gathering information and running the optimization process decreases. By increasing the number of customers in the system, more computation and storage are needed to store the customer's data and run the optimization process. The simulation results show that increasing the number of customers in the optimization problem also increases the execution time. To avoid high execution time, we propose to partition the entire system into distinct regions and solve the optimization problem at each region, separately. Thus, high scalability and fast response time will be achieved. At the end of the optimization process, the optimal schedule is sent to the customers and microgrids. The results given in Table III confirm that 1) when the number of regions is fixed, by

TABLE III
PROCESSING TIME UNIT FOR RUNNING THE WHOLE OPTIMIZATION
PROCESS AT DIFFERENT COMBINATION OF CUSTOMERS AND REGIONS

		Number of regions			
		1	5	10	15
Number of customers in each region	500	NA	89.5062	90.7032	91.2865
	1000	NA	179.0042	179.6313	186.3749
	2000	NA	359.1821	360.4404	373.9718
	10 000	1764.2	NA	NA	NA
	20 000	3517.8148	NA	NA	NA

704 increasing the number of customers in each region the conver-
705 gence time is increased linearly and 2) when the total number
706 of customers in the whole power system is fixed, by increasing
707 the number of regions and spreading the customers in different
708 regions, the convergence time is decreased significantly.

709 V. CONCLUSION

710 The DSM needs reliable and efficient communications, which
711 can be met by utilizing the multitier cloud computing based on
712 the software-defined infrastructure. In this architecture, edge
713 cloud provides cloud computing resources at the edge of the
714 network. The benefit of such an architecture is that it can pro-
715 vide a high level of scalability and reliability. In this paper,
716 we proposed a two-tier cloud-based model for the autonomous
717 DSM in the future SG in which the customer's power consump-
718 tion and microgrid resources are scheduled by the use of the
719 regional edge and core clouds, respectively, to reduce the cost
720 and improve the power grid performance. It has been shown
721 that spreading the customers in different regions reduces the
722 convergence time and improves the scalability. As the proposed
723 approach is able to provide online access to all customer power
724 consumption information and microgrid resources, so it can en-
725 able the dynamic DR optimization of the power consumption
726 and energy cost of the customers. Simulation results confirmed
727 that the proposed model reduces the cost for the customers and
728 improves the power grid in terms of peak load and peak-to-
729 average load ratio.

730 REFERENCES

731 [1] H. Arasteh *et al.*, "IoT-based smart cities: A survey," in *Proc. 16th IEEE*
732 *Int. Conf. Environ. Electr. Eng.*, Florence Italy, 2016, pp. 1–6.
733 [2] A. M. Kosek, O. Gehrke and D. Kullmann, "Fault tolerant aggregation for
734 power system services," in *Proc 2013 IEEE Int. Workshop Intell. Energy*
735 *Syst.*, Vienna, 2013, pp. 107–112.
736 [3] A. H. Mohsenian-Rad, V. W. Wong, J. Jatskevich, R. Schober, and
737 A. Leon-Garcia, "Autonomous demand-side management based on game-
738 theoretic energy consumption scheduling for the future smart grid," *IEEE*
739 *Trans. Smart Grid*, vol. 1, no. 3, pp. 320–331, Dec. 2010.
740 [4] I. Atzeni, L.G. Ordóñez, and G. Scutari, "Demand-side management
741 via distributed energy generation and storage optimization," *IEEE Trans.*
742 *Smart Grid*, vol. 4, no. 2, pp. 866–876, Jun. 2013.
743 [5] S. Maharjan, Q. Zhu, Y. Zhang, S. Gjessing, and T. Basar, "Dependable
744 demand response management in the smart grid: A stackelberg game
745 approach," *IEEE Trans. Smart Grid*, vol. 4, no. 1, pp. 120–132, Mar.
746 2013.
747 [6] H. Chen, Y. Li, R. H. Y. Louie, and B. Vucetic, "Autonomous demand side
748 management based on energy consumption scheduling and instantaneous
749 load billing: An aggregative game approach," *IEEE Trans. Smart Grid*,
750 vol. 5, no. 4, pp. 1744–1754, Jul. 2014.

[7] R. Deng, Z. Yang, J. Chen, N. Rahbari-Asr, and M.Y. Chow, "Resi-
751 dential energy consumption scheduling: A coupled-constraint game ap-
752 proach," *IEEE Trans. Smart Grid*, vol. 5, no. 3, pp. 1340–1350, May
753 2014.
754 [8] D. Li and S. K. Jayaweera, "Distributed smart-home decision-making in
755 a hierarchical interactive smart grid architecture," *IEEE Trans. Parallel*
756 *Distrib. Syst.*, vol. 26, no. 1, pp. 75–84, Jan. 2015.
757 [9] D.S. Markovic, D. Zivkovic, I. Branovic, R. Popovic, and D. Cvetkovic,
758 "Smart power grid and cloud computing," *Renewable Sustain. Energy*
759 *Rev.*, vol. 24, pp. 566–577, 2013.
760 [10] M. Shafie-khah *et al.*, "Optimal behavior of responsive residential de-
761 mand considering hybrid phase change materials," *Appl. Energy*, vol. 163,
762 pp. 81–92, 2016.
763 [11] I. Dusparic, A. Taylor, A. Marinescu, V. Cahill and S. Clarke, "Maximizing
764 renewable energy use with decentralized residential demand response,"
765 in *Proc. 2015 IEEE First Int. Smart Cities Conf.*, Guadalajara, 2015,
766 pp. 1–6.
767 [12] L. C. Siebert *et al.*, "Centralized and decentralized approaches to demand
768 response using smart plugs," in *Proc. 2014 IEEE PES Transmiss. Distrib.*
769 *Conf. Expo.*, Chicago, IL, USA, 2014, pp. 1–5.
770 [13] P. Siano and D. Sarno, "Assessing the benefits of residential demand
771 response in a real time distribution energy market," *Appl. Energy*, vol.
772 161, pp. 533–551, 2016.
773 [14] A. Sheikhi, M. Rayati, S. Bahrami, A. M. Ranjbar, and S. Sattari,
774 "A cloud computing framework on demand side management game in
775 smart energy hubs," *Electr. Power Energy Syst.*, vol. 64, pp. 1007–1016,
776 2015.
777 [15] M. Yigit, V. C. Gungor, and S. Baktir, "Cloud computing for smart grid
778 applications," *Comput. Netw.*, vol. 70, pp. 312–329, 2014.
779 [16] J.-M. Kang, T. Lin, H. Bannazadeh, and A. Leon-Garcia, "Software-
780 defined infrastructure and the SAVI testbed," in *Testbeds and Research*
781 *Infrastructure: Development of Networks and Communities*. New York,
782 NY, USA: Springer, 2014, pp. 3–13.
783 [17] R. Deng, Z. Yang, M. Chow, and J. Chen, "A survey on demand response
784 in smart grids: Mathematical models and approaches," *IEEE Trans. Ind.*
785 *Inform.*, vol. 11, no. 3, pp. 570–582, Jun. 2015.
786 [18] S. Bera, S. Misra, and J. J. P. C. Rodrigues, "Cloud computing applications
787 for smart grid: A survey," *IEEE Trans. Parallel Distrib. Syst.*, vol. 26, no. 5,
788 pp. 1477–1494, May 2015.
789 [19] H. Kim, Y. J. Kim, K. Yang and M. Thottan, "Cloud-based demand
790 response for smart grid: Architecture and distributed algorithms," in
791 *Proc. 2011 IEEE Int. Conf. Smart Grid Commun.*, Brussels, 2011,
792 pp. 398–403.
793 [20] K. S. Ng, C. S. Moo, Y. P. Chen, and Y. C. Hsieh, "Enhanced coulomb
794 counting method for estimating state-of-charge and state-of-health of
795 lithium-ion batteries," *Appl. Energy*, vol. 86, no. 9, pp. 1506–1511,
796 2009.
797 [21] J. Hofierka and J. Kaňuk, "Assessment of photovoltaic potential in urban
798 areas using open-source solar radiation tools," *Renew. Energy* vol. 34,
799 no. 10, pp. 2206–2214, Oct. 2009.
800 [22] C. Koch-Ciobotaru, L. Mihet-Popa, F. Isleifsson and H. Bindner, "Simu-
801 lation model developed for a small-scale PV system in distribution net-
802 works," in *Proc. 2012 7th IEEE Int. Symp. Appl. Comput. Intell. Inform.*,
803 Timisoara, 2012, pp. 341–346.
804 [23] R. G. Ross, "Flat-plate photovoltaic array design optimization," in *Proc.*
805 *14th IEEE Photovolt. Spec. Conf.*, 1980, pp. 1126–1132.
806 [24] K. Nishioka, T. Hatayama, Y. Uraoka, T. Fuyuki, R. Hagihara, and
807 M. Watanabe, "Field-test analysis of PV system output characteristics
808 focusing on module temperature," *Solar Energy Mater. Solar Cell*, vol.
809 75, no. 3–4, pp. 665–671, 2003.
810 [25] F. Kasten and G. Czeplak, "Solar and terrestrial radiation dependent on
811 the amount and type of cloud," *Solar Energy*, vol. 24, no. 2, pp. 177–189,
812 1980.
813 [26] J. A. Duffie and W. A. Beckman, "*Solar Engineering of Thermal Pro-*
814 *cesses*," 4th ed. Hoboken, NJ, USA: Wiley, 2013.
815 [27] "Solar PV maps and tools," 2016. [Online]. Available: [http://pv-](http://pv-map.apvi.org.au/)
816 [map.apvi.org.au/](http://pv-map.apvi.org.au/)
817 [28] R. G. Garroppo, S. Giordano, M. Pagano, and G. Procissi, "On traffic
818 prediction for resource allocation: a Chebyshev bound based allocation
819 scheme," *Comput. Commun.*, vol. 31, no. 16, pp. 3741–3751, 2008.
820 [29] IEM, "Iowa Environmental Mesonet (IEM)," 2016. [Online]. Available:
821 <https://mesonet.agron.iastate.edu>
822 [30] Office of Energy Efficiency, Natural Resources Canada, Energy Con-
823 sumption of Household Appliances Shipped in Canada Trends for
824 1990–2010, 2016. [Online]. Available: [http://www.nrcan.gc.ca/sites/](http://www.nrcan.gc.ca/sites/oeec.nrcan.gc.ca/files/pdf/publications/statistics/cama12/cama12.pdf)
825 [oeec.nrcan.gc.ca/files/pdf/publications/statistics/cama12/cama12.pdf](http://www.nrcan.gc.ca/sites/oeec.nrcan.gc.ca/files/pdf/publications/statistics/cama12/cama12.pdf)
826

827
828
829
830
831
832
833
834
835
836
837
838
839
840
841
842
843
844
845
846
847
848
849
850
851
852
853
854
855
856
857
858
859
860
861
862
863
864
865
866



Mohammad Hossein Yaghmaee Moghaddam (SM'12) received the B.S. degree from Sharif University of Technology, Tehran, Iran, in 1993, and the M.S. and Ph.D. degrees in communication engineering from Tehran Polytechnic (Amirkabir) University of Technology, Tehran, Iran, in 1995 and 2000, respectively.

From November 1998 to July 1999, he was with the Network Technology Group, C&C Media Research Labs., NEC corporation, Tokyo, Japan, as a Visiting Research Scholar. From

September 2007 to August 2008, he was with the Lane Department of Computer Science and Electrical Engineering, West Virginia University, Morgantown, WV, USA, as a Visiting Associate Professor. From July 2015 to September 2016, he was with the Electrical and Computer Engineering Department, University of Toronto, Toronto, Canada, as a Visiting Professor. Currently, he is a Full Professor at the Computer Engineering Department, Ferdowsi University of Mashhad, Mashhad, Iran. His research interests include SG communication, software defined networking, and network function virtualization.



Morteza Moghaddassian (S'15) received the M.S. degree in computer engineering from Ferdowsi University of Mashhad, Mashhad, Iran, in 2015. Since 2016, he is working toward the Ph.D. degree in electrical and computer engineering at the University of Toronto, ON, Canada.

He received the Edward S. Rogers Sr. departmental graduate fellowship. Prior to this, he was a Research Assistant at the Center of Excellence on Soft Computing & Intelligent Informa-

tion Processing, Ferdowsi University of Mashhad, Mashhad, Iran, where he successfully managed a research team to develop a social energy network application for the purpose of metering with built-in demand-response management modules, called "SocioGrid." His research interests include cloud computing, edge computing, resource monitoring and management, SG, and optimization of communication networks and open networking.



Alberto Leon-Garcia (F'99) received the B.S., M.S., and Ph.D. degrees in electrical engineering from the University of Southern California, Los Angeles, CA, USA, in 1973, 1974, and 1976, respectively.

From 1999 to 2002, he was the Founder and CTO of AcceLight Networks, Ottawa, ON, Canada, which developed an all-optical fabric multiterabit switch. Currently, he is a Professor in the Electrical and Computer Engineering Department, University of Toronto, ON, Canada.

His current research interests include application-oriented networking and autonomic resources management with a focus on enabling pervasive smart infrastructure.

Prof. Leon-Garcia is the author of the leading textbooks *Probability and Random Processes for Electrical Engineering* (Reading, MA, USA: Addison-Wesley, 1989) and *Communication Networks: Fundamental Concepts and Key Architecture* (New York, NY, USA: McGraw-Hill, 2006). He is a Fellow of the Engineering Institute of Canada. He received the 2006 Thomas Eadie Medal from the Royal Society of Canada and the 2010 IEEE Canada A. G. L. McNaughton Gold Medal for his contributions to the area of communications.

867
868
869
870
871
872
873
874
875
876
877
878
879
880
881
882
883
884
885
886
887
888
889

Queries

- | | |
|---|-------------------|
| Q1. Author: Please provide expansion of acronym "ToU." | 890 |
| Q2. Author: Please provide the subject in which the author "Mohammad Hossein Yaghmaee Moghaddam" received the B.Sc. degree. | 891
892
893 |

IEEE Proof